Stony Brook University

Basic Study on Degradation of nHAP-PLGA-Collagen – A Novel Biopolymer

A Thesis Presented

by

Liqiang Ren

to

The Graduate School

in Partial Fulfillment of the

Requirements

for the Degree of

Master of Science

in

Materials Science and Engineering

Stony Brook University

May 2016

Stony Brook University

The Graduate School

Liqiang Ren

We, the thesis committee for the above candidate for the

Master of Science degree, hereby recommend

acceptance of this thesis.

Rina (Irena) Tannenbaum
Professor, Department of Materials Science and Engineering, Program in Chemical and Molecular Engineering

T. Venkatesh
Associate Professor, Graduate Program Director (MSE), Department of Materials Science and Engineering

Sherif Abdelaziz
Assistant Professor, Department of Civil Engineering

This thesis is accepted by the Graduate School

Charles Taber
Dean of the Graduate School

Abstract of the Thesis

Basic Study on Degradation of nHAP-PLGA-Collagen – A Novel Biopolymer

by

Liqiang Ren

Master of Science

in

Materials Science and Engineering

Stony Brook University

2016

Bone tissue engineering is a rapidly developing field of interest. Bone scaffold materials have several applications of great importance including the fostering of healthy bone tissue and the repair of bone defects both in-vivo and in-vitro. Ideal scaffolds should be biocompatible, biodegradable, and promote cellular interactions and tissue development, and possess proper mechanical and physical properties [1]. nHAP-PLGA-Collagen is a novel synthesized block-polymer which has proved biocompatibility and mechanical properties. This thesis is focused on the degradation-controlling to fulfill the requirement of bone reconstruction and afterward digestion. The research focuses on internal and external factors which have effects on degradation time of nHAP-PLGA-Collagen. Internal factors include monomer ratio of D, L-lactide and glycolide monomers, porosity, and macro construction, which can modify the polymer. And external factors are temperature and pH impact the degradation of storage and during bone forming. In this thesis, nHAP-PLGA-Collagen block polymer has been characterized and been proven to have properties accounting for a bone scaffold material, including degradation adaptability.

Keywords: Bone scaffold, biodegradable polymer, degradation

Table of Contents

List of Figures

List of Table

List of Abbreviations

PLA ……...…….Poly(lactic acid)

PGA……poly(glycolic acid)

PLA……..poly(lactic-co-glycolide)

PLLA……...……..L-PLA

PDLA……...…….D-PLA

PDLLA/ PLGA……...……..D, L-PLA

nHAP……..……..……...Nanohydroapatite

nHAP-PLGA-Collagen…….....……..Nanohydroapatite-poly(lactic-co-glycolic acid)-collagen

TGA……..……...……...Thermogravimetric Analysis

FTIR……..……..…….... Fourier transform infrared spectroscopy

SEM…..……..……... Scanning Electron Microscope

Acknowledgments

This research was supported by Rina (Irena) Tannenbaum from Department of Materials Science and Engineering, Program in Chemical and Molecular Engineering, Stony Brook University. I thank my colleagues Shruti, Rick and Lyufei from Biomedical Nanomaterials Research Laboratory who provided insight and expertise that greatly assisted the research.

I thank Gwen, Fang Lu, Xianghao Zuo and Professor Miriam Rafailovich for assistance with SEM training, FTIR training and Tensile tester training, and Huafeng Huang, Jiaohao Huang and Hua Jiang for comments that greatly improved the manuscript.

I would also like to show my gratitude to the Maya for sharing her pearls of wisdom with us during the course of this research, and thank 3 committee reviewers for their insights and for their comments on an earlier version of the manuscript, although any errors are my own and should not tarnish the reputations of these esteemed persons.

Chapter 1

Introduction

1.1 Introduction of Bone Scaffold

1.1.1 Basic Concept of Bone Scaffold Materials

Bone grafting is a standard surgical practice, involving the replacement of deficient bone in order to repair bone fractures and bone defects caused by congenital disorders, traumatic injury or surgery of bone tumors [2]. In the recent decade, it has been estimated that 6.8 million fractures occur annually in the USA, resulting in an estimated $21 billion expenditure [3, 4]. However, the traditional grafts have their drawbacks. The main drawback of autografts is donor shortage. For allograft, the problem is the potential risk of transmitting diseases and immunological response [5]. In bone surgery for large bone defects or bone tumor resection, bone scaffolds have been a choice other than autografts and allograft [5]. Thus, tissue engineering which focuses on reliable bone scaffold will be the key to solving the bone defects repair dilemma. Also, this approach reduces the number of operations needed, resulting in a shorter recovery time for the patient [6].

Facing the complex biological and sensitive system of human body, the requirements of bone scaffold materials for bone tissue engineering are complicated and strict. First, biocompatibility of the substrate materials is imperative; that is the material must not elicit an unresolved inflammatory response nor demonstrate immunogenicity or cytotoxicity. Secondly, the mechanical properties of the scaffold must be sufficient and not collapse during handling and the patient's normal activities. As with all materials in contact with the human body, tissue scaffolds must be readily sterilizable to prevent infection [7]. Thirdly, a highly porous microstructure with interconnected pore networks is required to allow cell in-growth and reorganization. Also, materials should have appropriate surface chemistry to promote cellular attachment, differentiation, and proliferation. And finally, biodegradation is the highlight of some kinds of scaffold materials. Materials require controlled degradation consistent with sufficient structural integrity until the newly grown tissue has replaced the scaffold's supporting function.

Nowadays, bone scaffold materials are mainly developed in their branches – bioactive ceramic phases, biodegradable polymer matrices and composite scaffolds.

1.1.2 Bioactive ceramic phase

Bioactive glasses and ceramics have a common characteristic which is a time-dependent kinetic modification of the surface that occurs upon implantation. The surface forms a biologically active hydroxycarbonate apatite (HCA) layer which provides the bonding interface with tissues. The HCA phase that forms on bioactive implants are chemically and structurally equivalent to the mineral phase in bone providing interfacial bonding [8, 9]. The in vivo formation of an apatite layer on the surface of a bioactive ceramic can be reproduced in a protein-free and acellular simulated body fluid (SBF), which is prepared to have an ion concentration nearly equal to that of human blood plasma [6].

Bioactivity, however, is not an exclusive property for bioactive glasses. For application in tissue engineering, bioactive glasses are also supported enzyme activity [10-12]; vascularization [13, 14]; foster osteoblast adhesion, growth, differentiation; and induce the differentiation of mesenchymal cells into osteoblasts[15-17]. 45S5 Bioglass® is a typical representative of this class of materials. This material upregulates the gene expression that control osteogenesis and the production of growth factors[18]. The basic constituents of the most bioactive glasses are SiO_2, Na_2O, CaO, and P_2O_5. 45S5 Bioglasss contains 45% SiO_2, 24.5% Na_2O, 24.4% CaO and 6% P_2O_5, in weight percent [9]. Silicon has been found to play a key role in the bone mineralization and gene activation, which has led to an increased interest in the substitution of silicon for calcium into synthetic HA. Investigations in vivo have shown that bone ingrowth into silicon-substituted HA granules was remarkably greater than that into pure HA [6, 19]. The major drawback of this material is their low fracture toughness and mechanical strength, especially considering the porosity requirement.

Another representative bioactive ceramics is calcium phosphates. Around 60 wt% of bone is made of HA $Ca_{10}(PO_4)_6(OH)_2$ and therefore it is evident why HA and related calcium phosphates (e. g. α-TCP, β-TCP) have been intensively investigated as the major component of scaffold materials for bone tissue engineering [20-23].

1.1.3 Biodegradable Polymer Matrices

There are two types of biodegradable polymers: natural-based materials and synthetic biodegradable materials. The natural-based materials are one category, including polysaccharides (starch, alginate, chitin/chitosan, hyaluronic acid derivatives) or proteins (soy, collagen, fibrin gels, silk) and, as reinforcement, a variety of biofibers such as lignocellulosic natural fibers; and the other category is biodegradable polymers, which could be produced under controlled conditions and therefore exhibit in predictable and reproducible mechanical and physical properties such as tensile strength, elastic modulus and degradation rate [24-27]. Table 1.1 gives an overview of often used biodegradable polymers.

Table 1.1
Physical properties of synthetic, biocompatible, and biodegradable polymers used as scaffold materials[6]

Polymer	Melting point T_m (℃)	Glass transition point Tg (℃)	Biodegradation time (months)	Compressive* or tensile strength (MPa)	Modulus (GPa)
PLGA	Amorphous	45-55	Adjustable: 1-12	41.4-55.2	1.4-2.8
PGA	225-230	35-40	6-12	Fibre: 340-920	Fibre: 7-14
PLLA	173-178	60-65	>24	Pellet: 40-120 Film or disk: 28-50	Film or disk: 1.2-3.0
PCL	58	-72	>24		
PDLLA	Amorphous	55-60	12-16	Pellet: 35-150 Film or disk: 29-35	Film or disk: 1.9-2.4

Poly(lactic acid) (PLA) and poly(glycolic acid) (PGA), as well as poly(lactic-co-glycolide) polymers, are saturated poly-α-hydroxy esters which are the most often utilized biodegradable synthetic polymers for 3D scaffold[24, 28-30]. PLA exists in three forms: L-PLA (PLLA), D-PLA (PDLA), and the racemic mixture of D, L-PLA (PDLLA), and so as PLGA.

Degradation of these polymers is through de-esterification, according to the chemical properties of these polymers. Biodegradable polyester degradation occurs by uptake of water followed by the hydrolysis of ester bonds. Different factors affect the degradation kinetics, such as: chemical composition and configurational structure, processing history, molar mass (Mw), polydispersity (Mw/ Mn), environmental conditions, stress and strain, crystallinity, device size, morphology (e.g. porosity) and chain orientation, distribution of chemically reactive compounds within the matrix, additives[31, 32], presence of original monomers and overall hydrophilicity. Once degraded, the monomeric components of each polymer are removed by natural pathways. The body already contains highly regulated mechanisms for completely removing monomeric components of lactic and glycolic acids[6]. PLA and PGA can be processed easily and their degradation rates, physical and mechanical properties are adjustable over a wide range by using various molecular weights and copolymers[33]. And

according to Table 1.1, the degradation rates decrease in the following order: PGA> PDLLA> PLLA> PCL.

Thus, copolymers as PLGA has a wide range of degradation rates. The degradation kinetics are governed by both hydrophobic/hydrophilic balance and crystallinity. The composition of chains determines the degradation rate of PLGA polymers. Blends containing the greatest amount of PGA have been shown to degrade faster. On the other hand, PCL can take several years to degrade in vivo[34]. This thesis discusses the degradation mechanism and the rate controlling based on a novel synthesized degradable block-polymer material: nHAP-PLGA-Collagen.

1.2 nHAP-PLGA-Collagen

1.2.1 Background

Nanohydroapatite-poly(lactic-co-glycolic acid)-collagen (nHAP-PLGA-Collagen) is a kind of novel synthesized block-polymer. This kind of bone scaffold material has significant improvements on biocompatibilities and mechanical properties. At present, there is no synthetic bone graft substitute materials could reach similar biological and mechanical properties compared to bone itself. Hydroxyapatite (HAP) bioceramic, as a clinical bone graft substitute material, is only suitable for repairing small fractures or non-load-bearing bone defects because of its brittleness, low mechanical strength, and weak fatigue resistance. On the other hand, biodegradable polymers such as poly(L-lactide) (PLLA) have high elasticity but far less tensile strength. Therefore, the combination of polymer matrices and hydroxyapatite bioceramic enhanced mechanical properties complementarily. However, lacking interfacial bonding limits load transfer from the matrix to the inorganic moiety resulted in a phase separation at the polymer-filler interface [35, 36]. D. Bhuiyan et al. [37] solved this problem by nano using hydroxyapatite particles as initiators of polymerization and synthesized a novel polymer nHAP-PLGA copolymer, expressed as the equation below [37]:

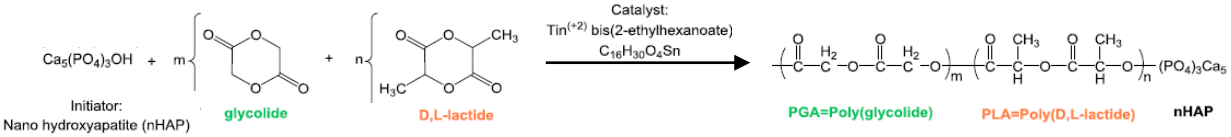

Besides, hydroxyapatite is the main inorganic component of bone tissues, which has good biocompatibility. On the other hand, organic components of bone, mainly collagen, would behave as a compliant material with high toughness, low modulus, and other properties

characteristic for polymers [38]. Collagens having suitable properties such as biodegradability, bioabsorbability with low antigenicity, high affinity to water and the ability to interact with cells through integrin recognition, are a very promising candidate for such a modification of the polymer matrix. It will fulfill requirements of possible strategies that would consist of the surface modification of the polymer matrix in order to enhance certain surface properties such as hydrophilicity or chemical compatibility. Furthermore, collagen would be to tether to the polymer a biological macromolecule, which, if properly chosen, would assist with both the compatibilization between the polymer matrix and the HAP moiety and with the integration with the surrounding tissue [39-42]. Collagen modification could be shown in following equation [37]:

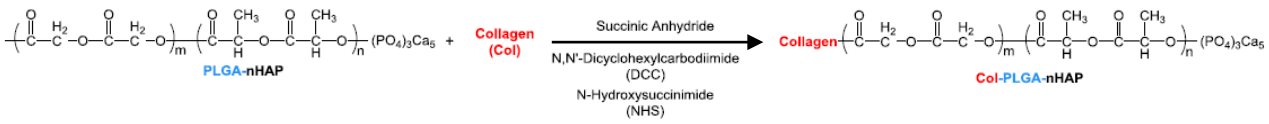

The polymer system described above need sufficient strength and toughness for bone tissue engineering applications. Bonding between all the components of the multi-phase system is required to obtain a mechanically and thermally stable material, preventing unexpected separation at the composite filler–polymer interface.

1.2.2 Mechanical and Thermal Stability Characterization

DSC was used to evaluate material crystallinity and the presence of distinct phases, and TGA was run to assess thermal stability.

DSC curve showed second heating cycle of the nHAP-PLGA polymer during the synthesis after coupling with succinic anhydride. Traditional ring-opening polymerization synthesis with dodecanol as the initiator. Melting temperatures were absent in both curves, supporting the fact that the PLGA polymer is amorphous. Both samples have similar glass transition temperature, in the range of 36-49 $^{\circ}C$. This result indicates that the PLGA polymer was grafted successfully on the surface of the nHAP initiator nanoparticles and the polymer that was generated using our novel synthesis had similar physical properties to PLGA copolymer that was made by the ring-opening polymerization using dodecanol as initiator.

The DSC curve of the first heating cycle of the nHAP-PLGA-collagen block-polymer exhibits a T_m at 113 $^{\circ}C$, which implies that the block-polymer possesses some degree of crystallinity compared to the PLGA polymer at the previous stage of synthesis, and a second transition at 174 $^{\circ}C$, most likely due to chain misalignment. For the sake of comparison, the

DSC curve of the first heating cycle of calf skin collagen type I, exhibits a T_m at $125\,^{\circ}C$ and a very small secondary transition at ~$240\,^{\circ}C$. These results indicate that after the addition of the collagen to the PLGA copolymer, the physical properties and the morphology of the polymer system change significantly. Firstly, the tethering of the collagen to nHAP-PLGA copolymer introduced a measurable crystalline phase as compared to the PLGA alone, as evidenced by the presence of a notable melting transition. Secondly, the considerable second transition of the nHAP-PLGA-collagen system suggests that the tethering of the collagen moiety induced the formation of either an aligned phase within the copolymer, or a secondary crystalline phase [43].

The nHAP-PLGA-collagen block-polymer obtained from a sample retrieved 45 min after the start of the collagen addition process. The curve shows that there was a modest weight loss at low temperatures, represented absorbed solvent. In order to determine the decomposition temperature of the various samples, three different tangents were drawn on both sides of each curve and averaged over nine different such measurements for each sample.

The copolymers obtained after the first two steps of the synthesis process, i.e. nHAP-PLGA copolymer coupled with succinic anhydride and after activation with NHS and DCC, exhibited decomposition temperatures below $330\,^{\circ}C$. However, after adding collagen, the decomposition temperatures measured at different time intervals increased significantly. The decomposition temperature of the collagen-containing copolymers increased to ~$370\,^{\circ}C$ immediately upon the addition of the collagen, and it remained constant during the reaction process. Given the fact that the decomposition temperature of calf skin collagen type I alone was only $310\,^{\circ}C$, it is clear that tethering the collagen to the PLGA copolymer has had a profound effect on the thermal stability of the hybrid material, beyond what would have been expected by assuming a simple composite effect. It is very likely that the attachment of the collagen to the PLGA polymer has intimately altered the morphology of the copolymer, which in turn has enhanced the thermal properties compared to the nHAP-PLGA copolymer and the collagen itself. This result is consistent with the result from DSC experiments. [37]

DMA was used for mechanical test in the work of Bhuiyan, D. et al. [37] Strength and flexibility are two particularly important properties of the complex biomaterial. From moduli and stress response of the nHAP-PLGA and the nHAP-PLGA-collagen samples as a function of strain, the nHAP-PLGA sample is stiffer (has higher modulus) at small strains than the nHAP-PLGA-collagen sample; however, it is less flexible and cannot sustain strains above 8%. Moreover, the modulus of this material decreased drastically, thus exhibiting a behavior

consistent with a brittle profile. Conversely, the nHAP-PLGA-collagen material was capable of sustaining relatively high and constant stresses over a broad range of strains, which renders the material quite ductile. This behavior is consistent with the fact that the collagen is thought to act in this system as a cross-linking agent, generating a hydrogel-like material that exhibits stronger and more flexible properties. nHAP-PLGA-collagen has an ultimate tensile strength of 2.62 MPa, which is close to the range of human cancellous bone of 7–20 MPa [44-46] and 300 times higher than the strength of pure collagen (10-12 kPa) [47], the latter having been tried clinically to enhance bone healing. nHAP-PLGA-collagen has higher strength compared to hydrogels made of chitosan (1-3 kPa), gelatin (2.5 MPa) and self-assembled peptide amphiphiles [48-50], which in turn are also investigated as bone graft substitutes. In addition, the flexible behavior of nHAP-PLGA-collagen, which is able to withstand high stresses over a wide range of strains, makes this material a more suitable candidate compared to ceramic materials (such as HAP, tricalcium phosphate, demineralized bone matrix and bioactive glasses), which are similarly studied for possible applications as bone graft material.

This result from thermal characterization indicates that the attachment of collagen improved the thermal properties of the copolymer, which essentially improve the mechanical properties of the novel copolymer. The mechanical analysis revealed that the material has a tensile strength comparable to human cancellous bone and has favorable modulus value for using as bone graft material.

1.3 Research of Degradation and Bone Regeneration

1.3.1 Bone Regeneration

The skeleton is a highly specialized and dynamic organ that undergoes continuous regeneration. It consists of highly specialized cells, mineralized and unmineralized connective tissue matrix, and spaces that include the bone marrow cavity, vascular canals, canaliculi, and lacunae. During development and growth, the skeleton is sculpted to achieve its shape and size by the removal of bone from one site and deposition at a different one; this process is called modeling [51]. Once the skeleton has reached maturity, regeneration continues in the form of a periodic replacement of old bone with new at the same location [52].

Fracture healing involves intracellular and extracellular molecular signaling for bone induction and conduction. It is a multistage repair process that follows a definable temporal and spatial sequence [53-56]. Molecular mechanisms known to regulate skeletal tissue formation

during embryological development are recapitulated during fracture healing [57]. Many local and systemic regulatory factors, including growth and differentiation factors, hormones, cytokines, and extracellular matrix, interact with several cell types, including bone and cartilage forming primary cells or even muscle mesenchymal cells, recruited at the fracture-injury site or from the circulation [58]. During the repair process, the way of normal embryonic development is recapitulated with the coordinated participation of several cell types [57]. There are four components involved in the injury site, including the cortex, the periosteum, the bone marrow, and the external soft tissues, contribute in the healing process at different extent, depending on multiple parameters present at the injured tissue such as growth factors, hormones and nutrients, pH, oxygen tension, the electrical environment and the mechanical stability that have been obtained [59, 60]. In classical histological terms, fracture healing has been divided into direct (primary) and indirect (secondary) fracture healing. Integrated cellular events, and their temporal and spatial characteristics, have been elucidated by using a model of experimental fracture healing in the rat [54].

Direct cortical fracture healing

Direct fracture healing occured only when there is anatomic reduction of the fracture fragments by rigid internal fixation and decreased intrafragmentary strain [61]. This process involves a direct attempt by the cortex to reestablish new Haversian systems by the formation of discrete remodeling units known as 'cutting cones', in order to restore mechanical continuity [61]. Vascular endothelial cells and perivascular mesenchymal cells provide the osteoprogenitor cells to become osteoblasts. During this process, little or no periosteal response is noted (no callus formation) [54].

Table 1.2. Timing of cellular events and expression of signaling molecules during murine fracture healing [53, 58, 62, 63].

Days	Cellular events	Expression of signaling molecules
Day 1	Haematoma formation, inflammation	Cytokines: IL-1, IL-6, TNF-α released by inflammatory cells
	Recruitment of mesenchymal cells	
	Osteogenic differentiation of MSCs from bone marrow	PDGF, TFG-beta released from degranulating platelets
		BMP-2 expression and restricted to day 1 expression of GDF-8
Day 3	MSCs proliferation begins	Decline of cytokines levels
	Proliferation and differentiation of	Expression of TGF-β2, -β3, GDF-10, BMP-5, -6

	preosteoblasts and osteoblasts in regions of intramembranous ossification Angiogenesis begins	Angiopoietin-1 is induced
Day 7	Peak of cell proliferation in intramembranous ossification between days 7 and 10 Chondrogenesis and endochondral ossification begin (days 9-14 maturation of chondrocytes)	Peak of TGF-β2 and -β3 expression Expression of GDF-5 and probably GDF-1
Day 14	Cessation of cell proliferation in intramembranous ossification, but osteoblastic activity continues Mineralization of the soft callus, cartilage resorption, and woven bone formation Neo-angiogenesis which infiltrates along new mesenchymal cells Phase of most active osteogenesis until day 21	Decreased levels of expression for TGF-β2, GDF-5, and probably GDF-1 Expression of BMP-3, -4, -7, and -8 VEGFs expression Second increase of IL-1 and TNF-α which continues during bone remodelling
Day 21	Woven bone remodelled and subsequently replaced by lamellar bone	Decreased expression of TGF-β1 and TGF-β3, GDF-10, and BMPs

Indirect fracture healing

The majority of fractures heal by indirect fracture healing. It involves a combination of intramembranous and endochondral ossification with the subsequent formation of a callus [54]. It is generally enhanced by motion and inhibited by rigid fixation [61]. Intramembranous ossification involves the formation of bone directly, without first forming cartilage, from committed osteoprogenitor and undifferentiated mesenchymal cells that reside in the periosteum, farther from the fracture site [54]. It results in callus formation, described histologically as 'hard callus' [54]. In this type of healing, the bone marrow's contribution to the formation of bone is during the early phase of healing, when endothelial cells transform into polymorphic cells, which subsequently express an osteoblastic phenotype [64].

Endochondral ossification involves the recruitment, proliferation, and differentiation of undifferentiated mesenchymal cells into cartilage, which becomes calcified and eventually replaced by bone. Its temporal characteristics include six identifiable stages including an initial stage of haematoma formation and inflammation, subsequent angiogenesis and formation of cartilage, cartilage calcification, cartilage removal, bone formation, and ultimately bone remodeling [54]. This type of fracture healing, is contributed from the adjacent to the fracture periosteum and the external soft tissues, providing an early bridging callus, histologically

characterized as ‘soft callus’, that stabilizes the fracture fragments [54].

The classification of fracture healing in direct and indirect healing reflects the histological events that occur during the repair process. However, the ongoing research in bone regeneration provided a further understanding of the cellular and molecular pathways that govern these events, by demonstrating the existence of various signaling molecules and elucidating their contribution in the initiation and control of this physiological process at the molecular level.

Pioneering studies both in vivo and in vitro showed that bone regenerating time related to defect size and scaffold material [5, 65-67]. And properties of scaffolds determine bone regenerating mechanism and facilitate vascular invasion and bone development. For example, pore sizes less than 15-50 μm result in fibrovascular ingrowth, pore sizes of 50-150 μm encourage osteoid formation, and pore sizes greater than 150 μm encourage the ingrowth of mineralized bone [68]. Ideally, the scaffold should be resorbed at a rate commensurate with new bone formation: dissolved scaffold is dissolved by multinucleated giant cells. Thus, adjustably degradable scaffolds are essential in tissue engineering.

Though under different regenerated time, primary osteoblast proliferation is certainly determined at 24 hours, 3, 7, 14 and 21 days [69]. The time of cellular events and expression of signaling molecules during murine fracture healing is shown in Table 1.1. Therefore, a degradation monitoring for 21 days is the basic standard to investigate degradation process, which is taken in this thesis.

1.3.2 Polymeric Scaffold Degradation

As mentioned above, biodegradation rate of polymer matrices is tunable in repair or regeneration process of tissue. And this is usually achieved by adjusting the composition of the polymers. In PLGA polymer, the more glycolic monomers polymer has, the higher degradation rate it presented. Degradation in vitro of 3D porous PLGA scaffold is reported by Linbo et al. [70]. In their work, PLGA 85/15, PLGA 75/25 and PDLLA are carried out in PBS solution under pH 7.4 at 37 $^{\circ}C$ for up to 26 weeks. During this process, PDLLA scaffold could survive the 26-week intact, and the PLGA 85/15 outlasted the PLGA 75/25 scaffold. Change of the diameter and height of PLGA 85/15 demonstrate the degradation procedure visually.

Dimensions of D/D_0 and H/H_0 are recorded in the 26 weeks. A decrease of 4-8% was observed within 2 weeks of all the scaffolds, and then stay unchanged before week-8. Dramatically decreasing happened after 8 weeks, which led to neck down of cylindrical

scaffolds. At the final stage of degradation, the cylindrical PLGA scaffolds caved in at the middle part with the caved-in part becoming soft, non-porous polymer [70].

Mechanical properties are significant parameters during evaluating a certain scaffold. Linbo et al pointed out that the mechanical properties, such as compressive yield stress and elastic modulus, would increase remarkably in early stage of degradation. Then, a corresponding decrease in modulus was observed after 11 and week 6 for PLGA 85/15 and PLGA 75/25 scaffolds respectively. Wu et al. test compressive yield stress σ_y and elastic modulus E [70]. Similarly, PDLLA kept its mechanical properties during the 26 weeks-degradation test. PLGA 75/25 lost it compressive yield stress and elastic modulus more rapid than PLGA 85/15. The early stage is characterized by an increase of mechanical properties but a decrease of the dimensions of scaffolds while the weight remained constant. This phenomenon has been reported by Zhang et al. that modulus of PLGA foams gradually increased because the porosity of the foams decreased [71]. Dimension shrinkage might lead to change of porosity and diminishment of some structural defects in the porous sample.

SEM images give a visual proof of porous collapse [70]. Original scaffold has relatively uniform pore morphology. For the first 14 weeks, no significant morphological change was observed microscopically. When degraded for 20 weeks, the number and size of the pores both decreased and some fiber-like connection appeared among the pores. At 24 weeks, most of the pores vanished and the remaining pores were smaller. When degraded for 20 weeks, the size of some pores diminished, and some pore wall disappeared and bigger pores thus formed. At 24 weeks, the central part of the scaffold became soft non-porous polymer but there were still some small pores with thicker wall at the periphery of the samples. The changes of pore morphology on PLGA 75/25 was similar but happened earlier as it degraded faster [70].

This study on similar polymer matrices materials gives guidance on investigating novel synthesized biodegradable material – nHAP-PLGA-Collagen. The formulation of polymer is the major factor effected degradation rate. And other factors in control such as temperature, pH, and enzyme have not been discussed yet.

1.4 Project Basis and Significance

This research studied degradation progress of nHAP-PLGA-Collagen materials and focused on control the degradation rate through control monomer ratio, pH and temperature. Lactic acid and glycolic acid monomers at ratio of 75: 25 and 50: 50 are polymerized using

nanohydroapatite as initiator and modified with type I collagen. Samples are stored under $4^{\circ}C$ and $37^{\circ}C$ in pH 6.4, pH 7.4 and pH 8.4 PBS buffer. Degradation was monitored by TGA, FTIR, SEM and tensile tester. TGA ramp showed transition step changes. Through studying function between critical temperatures and gravimetric loss to know the loss of components. Decreasing intensity of characteristic peak in FTIR gave an idea of changes on functional groups' vibration which present the degradation of polymer. SEM and tensile tester characterized direct-viewing impression parameters of morphology and mechanical properties on materials' degradation.

As a novel synthesized porous scaffold material, degrading mechanism of nHAP-PLGA-Collagen block-polymer need to be investigated so that it can be tunable in repair or regeneration process of tissue, as promising bone scaffold material in tissue engineering.

Chapter 2

Nanohydroapatite-PLGA-Collagen Block-Polymer Synthesis

2.1 Background

Nanohydroapatite-PLGA-Collagen is synthesized to meet requirements of biocompatibilities and mechanical strength. In this study, we developed a novel synthesis method to create a complex collagen-based biopolymer that promises to possess the necessary material properties for a bone graft substitute. The synthesis was carried out in several steps. In the first stage, a ring-opening polymerization reaction initiated by hydroxyapatite nanoparticles was used to polymerize D,L-lactide and glycolide monomers to form poly(lactide-co-glycolide) copolymer. In the second stage, the polymerization product was coupled with succinic anhydride, and subsequently was reacted with N-hydroxysuccinimide in the presence of dicyclohexylcarbodiimide as the cross-linking agent, in order to activate the copolymer for collagen attachment. In the third and final stage, the activated copolymer was attached to calf skin collagen type I, in hydrochloric acid/phosphate buffer solution and the precipitated copolymer with attached collagen was isolated. The synthesis was monitored by infrared spectroscopies, and the products after each stage were characterized by thermal and mechanical analysis.

Those results show the functional groups' changes in each stage and reveal the patterns and phases change during polymerization and modifications.

2.2 Experiments

2.2.1 Reagents and Instruments

The reagents and instruments used for experiments in this chapter are listed in table 2.1 and table 2.2.

Table 2.1 Information of reagents used in chapter 2

Reagents	Purity	Manufacturer	Other information
DL-Lactide	99%	Alfa Aesar	
Glycolide	≥99%	Sigma Life Science	
Succinic anhydride	≥99%	Aldrich Chemistry	
Collagen from calf skin	/	Sigma Life Science	Solid
Hydroxyapatite	≥97%	Aldrich Chemistry	<200 nm nanopowder
N-Hydroxysuccinimide	98%	Aldrich Chemistry	
DCC	99%	Aldrich Chemistry	
Methylene Chloride	Anhydrous	Spectrum	
Tin(II) 2-ethylhexanoate	92.5-100.0%	Sigma Life Science	
Diethyl ether	≥99%	Sigma-Aldrich	Contains BHT as inhibitor
Ethyl acetate	99.8%	Sigma-Aldrich	
Toluene	99.8%	Sigma-Aldrich	
N,N-Dimethylformamide	99.8%	Sigma-Aldrich	
Sodium phosphate dibasic heptahydrate	98.0-102.0%	Sigma-Aldrich	
Sodium phosphate monobasic monohydrate	≥98%	Sigma-Aldrich	

Table 2.2 Information of instruments used in chapter 2

Instruments	Model/Cat. No.	Manufacturer
Heating Mantle	100AO402	Glas-Col
Advanced Multiparameter Controller	TC9500	Cole Parmer OAKTON Electrochem
Advanced Hotplate Stirrer	11626262	Fisher Scientific
Analytical Balance	E64i1s	Sartorius
Thermogravimetric Analysis	Q500	TA Instruments
FT-IR Spectrometer	Nicolet iS50	Thermo Scientific

2.2.2 Experiment Methods

Polymerization of PLGA initiated by nHAP

Reagents were designed to polymerize using two different monomer ratio. In each sample, 0.168 g nanohydroapatite was dried overnight in a vacuum oven at $80^{\circ}C$ and further dried in a three neck flask at $100^{\circ}C$ for 30 min. The amount of D,L-lactide and glycolide monomers adding to flask are shown in Table 2.3. Mantle was set at $150^{\circ}C$ while stir bar spinning in flask. A condenser was connected to the middle neck of flask and was attached a nitrogen gas balloon on the top. One side neck was connected to a vacuum pump and the other was plugged by a glass stop. The reactor was purged with nitrogen gas three times and when

the monomers melted, mixture was sonicated with a sonicator probe for 5 min. After the temperature had reached 150$^{\circ}C$ solution of 0.01 g stannous octoate catalyst and 2 mL toluene was added to the flask. After 2 h of polymerization, the vacuum pump was opened to vacuum the pressure inside to 25 inHg for 30 min. Then 0.04 g succinic anhydride was added subsequently to obtain a carboxyl end group. The reaction ended after all period of 4.5 h of polymerization. Product of nHAP- PLGA copolymer and dried overnight in vacuum oven at room temperature and store at 4$^{\circ}C$. Monomers and product are characterized by FT-IR and TGA.

Table 2.3. Monomer ratio in polymerization

Sample #	Monomers	Ratio (%)	Mass (g)
1	D,L-lactide	75	7.5
	Glycolide	25	2.5
2	D,L-lactide	50	5
	Glycolide	50	5

Activation of nHAP-PLGA with n-hydroxysuccinimide

2 g of nHAP-PLGA was dissolved in 200 mL anhydrous methylene chloride. A solution of 0.078 g NHS and 0.018g DCC (30% excess) was added into dissolved nHAP-PLGA [39]. The reaction continued for 20 hours under nitrogen atmosphere. Then, polymer solution was dissolved in ethyl acetate and precipitated in anhydrous diethyl ether. The precipitated polymer which called nHAP-PLGA- NHS was collected in petri dish and dried in vacuum at room temperature overnight, stored at 4$^{\circ}C$.

Attachment of collagen to the PLGA copolymer

50 µL 37.5% concentrated hydrochloric acid is added to 500 mL distilled water, preparing 1mM HCl solution. Sodium phosphate dibasic heptahydrate ($Na_2HPO_4 \cdot 7H_2O$) and 0.779g sodium phosphate monobasic monohydrate ($NaH_2PO_4 \cdot H_2O$) was dissolved into 50 mL distilled water and verified with three-point calibrated pH meter for preparing 50mM pH 7.4 PBS buffer solution. 160 mL calf skin collagen type I was collected in 600 mL beaker in ice bath and was dissolved by 223.8 mL 1 mM HCl. After collagen completely dissolved, solution subsequently diluted with 300 mL 50 mM pH 7.4 PBS buffer. 0.96 g nHAP-PLGA-NHS polymer was dissolved in 26.6 mL anhydrous DMF and added dropwise to the collagen solution [39]. After 3 hours of reaction, the nHAP-PLGA-Collagen block-polymer was

centrifuged, molded and dried in vacuum oven at room temperature for 3 days. The molding steps will be expatiated in chapter 3. Samples were store at $4^{\circ}C$ until they were used in subsequent degradation experiment.

Characterization with FTIR

The samples for FT-IR absorption spectra were collected at room temperature at wavelength of 4000-400 cm^{-1}. One background is collected before sample signals. Every spectra is repeatedly collected 32 times under ATR mode for high resolution. Omnic software suite attached to the FTIR instrument was used for spectrum's analysis.

Measurements of thermal properties with TGA

The TGA could measure the mass range between 1mg to 1g. Samples were collected around 20 mg and heating up in platinum pan under nitrogen atmosphere. Ramp procedure was used in thermal behavior analysis, heating rate at $5^{\circ}C/\min$ from room temperature to $600^{\circ}C$.

2.3 Result and Discussion

2.3.1 Thermogravimetric Analysis

Polymers in each stage during synthesis showed differences thermogravimetry. The results of 50/50 polymer in three stages are shown in Figure 2.1. Temperature raised at 5 $^{\circ}C/\min$ from room temperature to $600^{\circ}C$. In each figure, left solvent is purged as impurities before $100^{\circ}C$. Afterward, a major ramp started at around 250-300 $^{\circ}C$ in all TGA profiles.

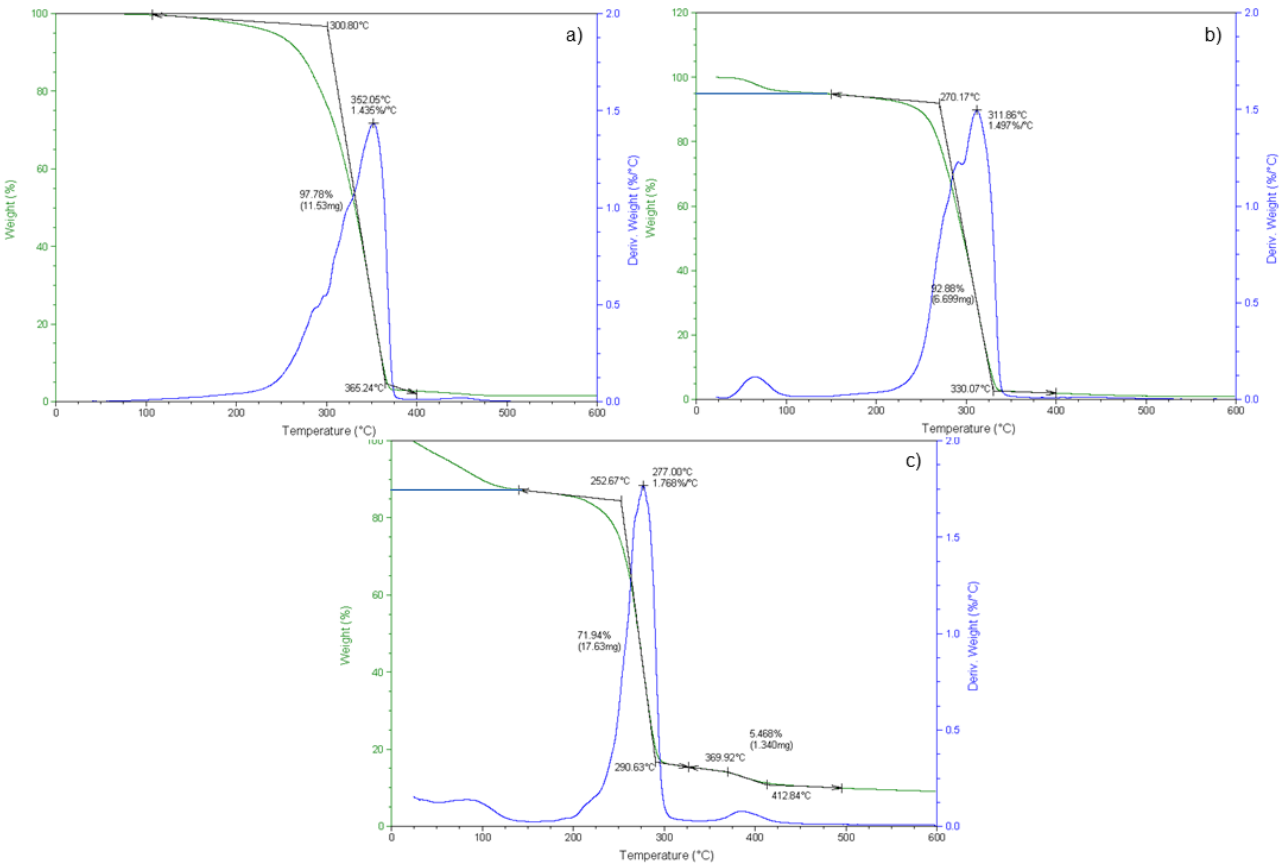

Figure 2.1. TGA profiles of 50/50 polymer a) nHAP- PLGA, b) nHAP-PLGA-NHS, c) nHAP-PLGA-Collagen, and transition analysis.

Compared to nHAP-PLGA-NHS, decomposition of undecorated nHAP-PLGA happened later. The major transition started at 300.80 $^{\circ}C$ and end at 365.24 $^{\circ}C$, and meanwhile, DTA reaches peak at 352.05 $^{\circ}C$, losing weight at rate of 1.435 %/ $^{\circ}C$. Though lost nearly same weight (excluding impurity, weight loss should be 92.88% / 95.00% ×100% = 97.76%), transition of nHAP-PLGA-NHS started and ended 30 $^{\circ}C$ earlier than undecorated polymer did, which proved a successful decoration as a corroborative evidence. The attachment of collagen further decreased the decomposition temperature of the polymer. Decomposition started at 252.67 $^{\circ}C$ and became two- step-transition. The first weight loss ended at 290.63 $^{\circ}C$ and lost 71.94% / 87% ×100% = 82.68% of the weight. And second transition during 369.92 $^{\circ}C$ to 412.84 $^{\circ}C$ lost 5.468% / 87% ×100% = 6.28%. Summing up the weight loss in two transitions, the total loss is 88.96% which is about 9% less than weight loss of former steps. In another word, residues in the profile of nHAP-PLGA-Collagen account for 9% more than those in nHAP-PLGA or nHAP-PLGA-NHS. A preliminary TGA test on calf skin Type I collagen shown in Figure 2.2. Excluding impurities, there are two major drops one from 152.87 $^{\circ}C$ to

183.92$^{\circ}C$ and the other from 276.25$^{\circ}C$ to 344.48$^{\circ}C$. The bigger one overlapped the major ramp in nHAP-PLGA-NHS TGA profile; however, this ramp in collagen profile ended around 500$^{\circ}C$ which resulted in the secondary ramp in nHAP-PLGA-collagen profile. And remarkably, the residue is 20.36%, far more than that in nHAP-PLGA-NHS of less than 5%, which result in an increasing residue in nHAP-PLGA-collagen.

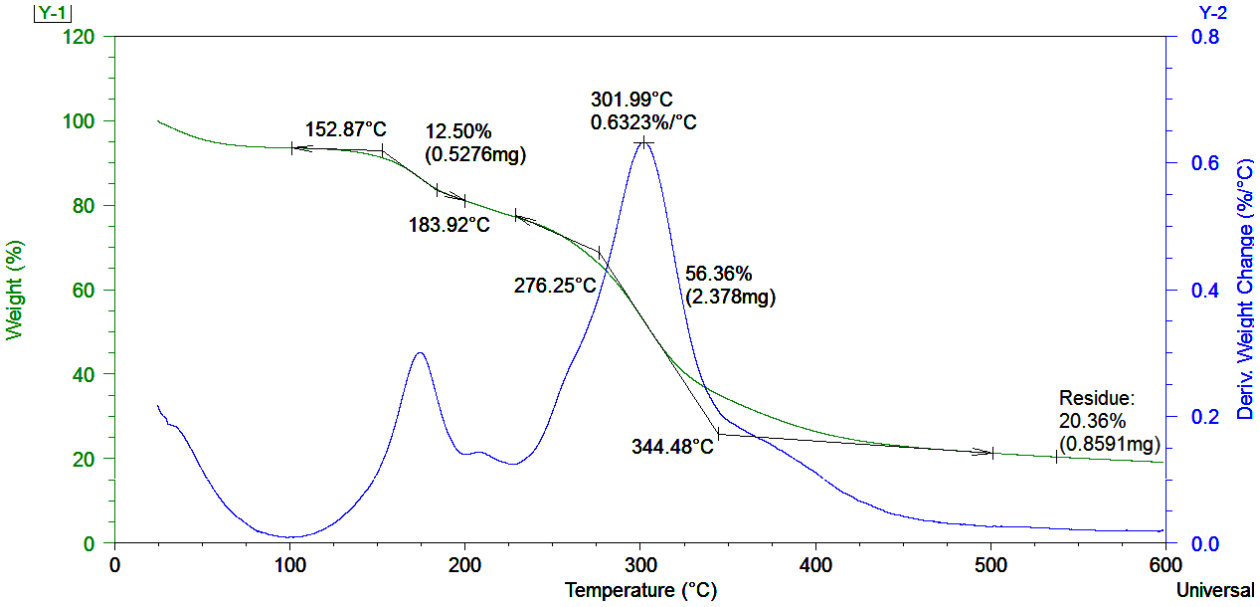

Figure 2.2. TGA profile of calf skin Type I collagen

The TGA profiles of 75/25 nHAP-PLGA-Collagen under three synthesis stage was shown in figure 2.3. Most changes among the three stages are similar to that of 50/50 polymer while collagen's attachment did not affect the thermal behavior of the main ramp. Still, a 5.5%-loss secondary ramp subsequently appear from 376$^{\circ}C$ to 420$^{\circ}C$.

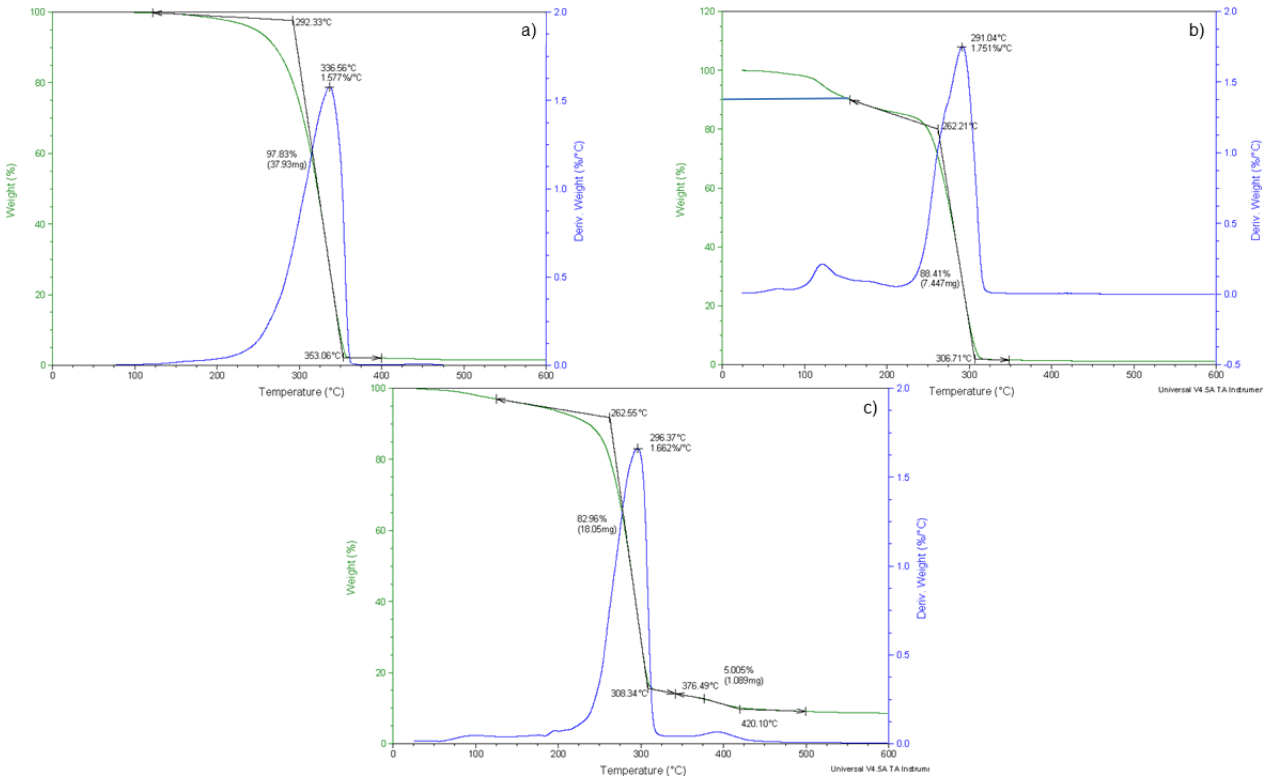

Figure 2.3. TGA profiles of 75/25 polymer, a) nHAP- PLGA, b) nHAP-PLGA-NHS, c) nHAP-PLGA-Collagen, and transition analysis.

Comparing 75/25 polymer and 50/50 polymer, weight change of this two kinds of polymers are the same at 98% at stage one. Residues are combination of unburned carbon and hydroxyapatite which has no gravimetric change up to $900^{\circ}C$, proven by preliminary tests. Initial decomposition started both at $100^{\circ}C$, and the final decomposition temperature is $500^{\circ}C$. However, during decomposition, there are some differences. From DTA graph, 50/50 HAP-PLGA-Collagen has a higher peak decomposition temperature at $352.05^{\circ}C$, while that of 75/25 HAP-PLGA-Collagen at $336.56^{\circ}C$. In all, 50/50 block-polymer has a higher heat resistant than 75/25 HAP-PLGA-Collagen at the first step. However, after decorating collagen in final stage, though sharing same thermal behavior, the decomposition temperature of 75/25 HAP-PLGA-Collagen is $10^{\circ}C$ higher than 50/50 HAP-PLGA-Collagen. Residue in first two stages is lower than 3%; however, it raised to around 10% in the third stage. The secondary peak and the increased amount of residue were because of introducing of collagen. It has a clear phase separation to nHAP-PLGA and has a higher phase transition temperature.

2.3.2 Fourier Transform Infrared Spectroscopy Characterization

Comparison of 75/25 and 50/50 nHAP-PLGA

The FTIR spectra shape of 75/25 and 50/50 is about the same from 4000 to 1500 cm^{-1}. Those are shown in Figure 2.4. And strongest two peaks at 1748 cm^{-1} and 1063 cm^{-1} for both of these two materials show the same intensity. While there are some differences. Based on 75/25, peak 1450 cm^{-1} and 1423 cm^{-1} switch their intensity on 50/50. Peak 1450 cm^{-1}, standing for scissors bending vibration of C-C, is much weaker than the same peak of 50/50, instead peak 1423 cm^{-1} increased. Peak 1423 cm^{-1} is also standing for scissors bending vibration C-C, while caused by Carbonyl conjugate effect. And there are some differences in details at fingerprint region. The FTIR spectra proofed that 50/50 has more C=O but less C-C, same as shown in the following block-polymer structure of nHAP-PLGA:

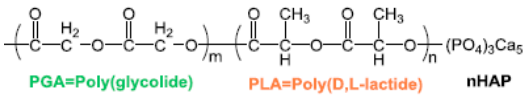

That is less fraction of Poly(D,L-lactide) (PLA) and more fraction of Poly(glycolide) (PGA).

Comparison of 75/25 and 50/50 nHAP-PLGA-NHS:

The comparison of stage 2 shown in Figure 2.5 is pretty similar to the spectra of stage 1, with proven larger fraction of PGA. Besides, the similar switch happened to peak 1083 cm^{-1} and peak 1038 cm^{-1} in fingerprint region, and peak at 570 cm^{-1} diminished. Peaks around 580 cm^{-1} represent ring in cycloalkanes which N,N'-Dicyclohexylcarbodiimide have. From this result, 75/25 is a better candidate for N,N'-Dicyclohexylcarbodiimide decoration.

Both of 50/50 and 75/25 show the same tendency from stage 1 to stage 2. Peak signal 580 cm^{-1} increased significantly, and peak signal 1251 cm^{-1} decreased. As mentioned, peak 580 stand for decorated functional groups and 1280-1150 cm^{-1} represents esters. Those broken ester bounds are replaced by new functional groups.

Collagen decoration

The spectra of collagen decorated are nearly the same to the spectra of stage 2, except a few peaks at 3311 cm^{-1}, 1628 cm^{-1} and 1545 cm^{-1}. At those position, the peaks represented the functional groups from collagen which are easy to identify in Figure 2.6.

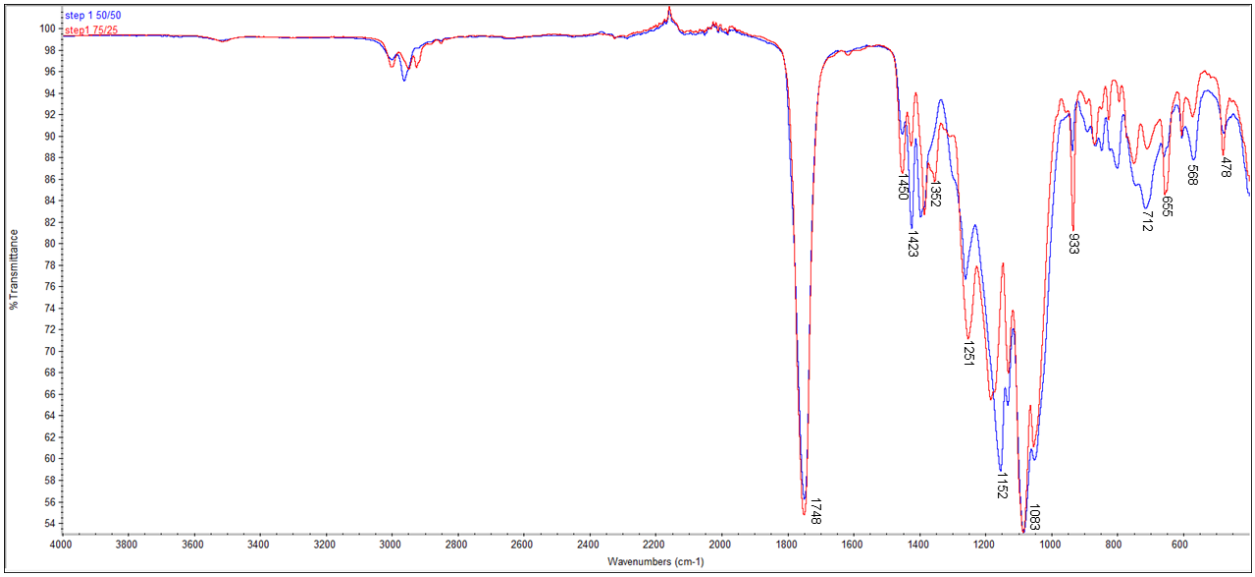

Figure 2.4. Comparison of 75/25 and 50/50 nHAP-PLGA in stage 1. The spectrum in red stand for 75/25 nHAP-PLGA and the spectrum in blue represent 50/50 nHAP-PLGA.

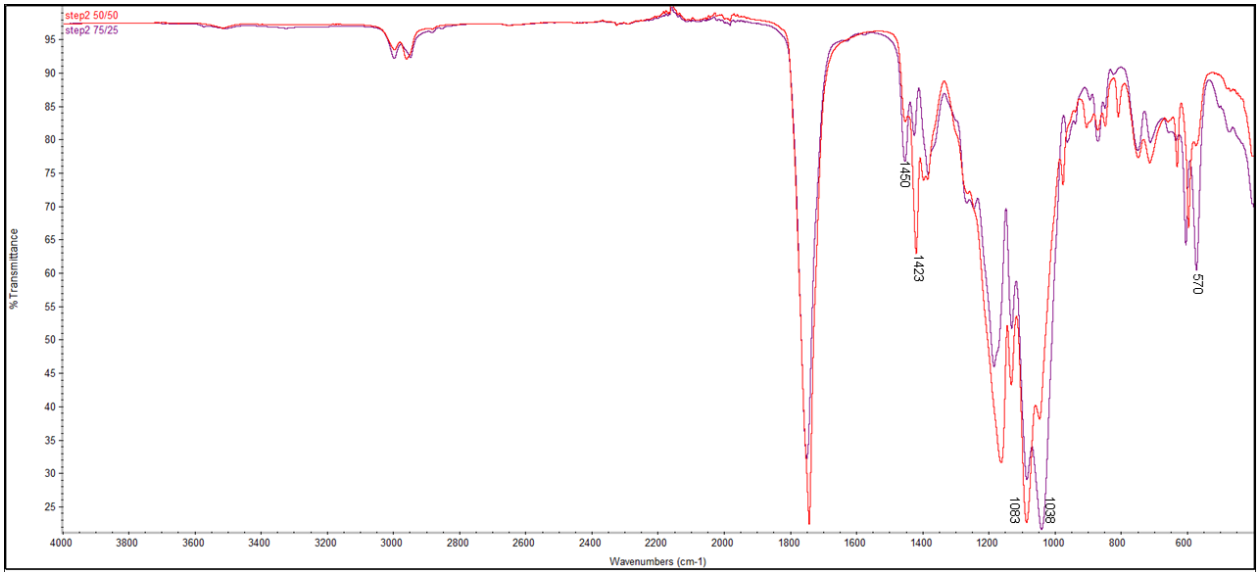

Figure 2.5. Comparison of 75/25 and 50/50 nHAP-PLGA-NHS in stage 2. The spectrum in purple stand for 75/25 nHAP-PLGA and the spectrum in blue represent 50/50 nHAP-PLGA.

Appeared new peaks in both of 50/50 and 75/25 nHAP-PLGA-Collagen spectra compared to their spectra at stage 2 matched the position in collagen. The introducing of Peak 3311 cm^{-1} and peak 1628 cm^{-1} represented $–NH_2$. Peak 2022 cm^{-1} and peak 1545 cm^{-1} proved existence of $>NH^{+}Cl$. Thus, this is a solid evidence to explain the successfully decoration of

collagen on copolymer. Also these spectra are used as initial data for degradation experiments in next steps.

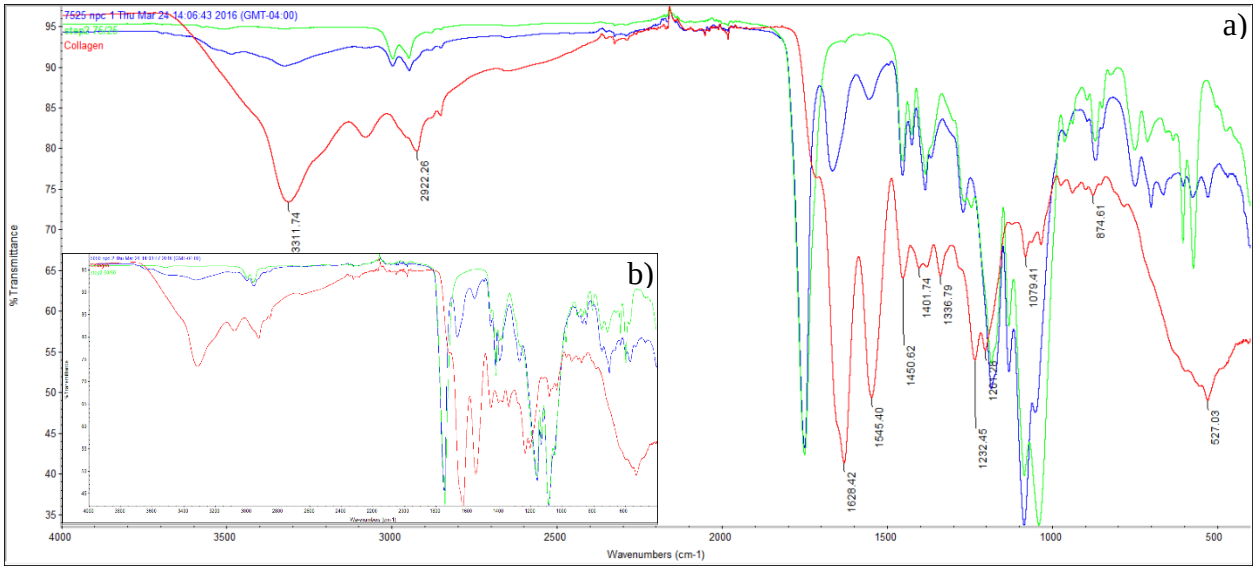

Figure 2.6. Spectra comparison among nHAP-PLGA-Collagen (blue), nHAP-PLGA-NHS (step 2) (green) and Collagen (red). a) Spectra comparison of 75/25-monomers-ratio block-polymer; b) Spectra comparison of 50/50-monomers-ratio block-polymer.

2.4 Conclusion

In this chapter, PLGA polymer was successfully polymerized using nHAP as initiator and decorated with collagen eventually. From thermogravimetric analysis, decoration of collagen lowered the decomposition temperature and introduced a secondary ramp because of collagen's higher completed decomposition temperature. And this part of weight loss can be used to monitor collagen degradation in following degradation experiments. The increasing intensity of peak 3311 cm^{-1}, 1628 cm^{-1}, 2022 cm^{-1} and 1545 cm^{-1} in FTIR spectra provided more distinct proofs explaining that collagen is bonded to nHAP-PLGA. And the peak 1423 cm^{-1} indicate the difference between 50/50 nHAP-PLGA-Collagen and 75/25 nHAP-PLGA-Collagen. 50/50 nHAP-PLGA-Collagen has a higher transmittance at 1434 cm^{-1}.

Chapter 3

Mold Design and Compression Forming

3.1 Background

To monitor the procedure of degradation, specimens should be uniform and suitable for subsequent test. Mechanical properties for bone scaffold is important, especially in early stages, in order to support patients on daily activities. Another factor need to concern is the water in precipitation. Water has a negative effect to samples when to apply compression, because it disperse pressure. Base on those factors, the chosen materials for mold should be able to absorb extra moisture and in certain shape.

A tensile specimen is a standardized sample cross-section. It has two shoulders and a gage (section) in between. The shoulders are large so they can be readily gripped, whereas the gauge section has a smaller cross-section so that the deformation and failure can occur in this area [72]. These specimens are usually named dog-bone specimens. These specimens may not be exact representation of the whole workpiece because the grain structure may be different throughout. In smaller workpieces or when critical parts of the casting must be tested, a workpiece may be sacrificed to make the test specimens [72]. For workpieces that are machined from bar stock, the test specimen can be made from the same piece as the bar stock.

Gypsum plaster, or plaster of Paris, is produced by heating gypsum to about 300 °F (150 °C) and is a feasible materials for mold:

$CaSO_4 \cdot 2H_2O + heat \rightarrow CaSO_4 \cdot 0.5H_2O + 1.5H_2O$ (released as steam)

When the dry plaster powder is mixed with water, it re-forms into gypsum. The setting of unmodified plaster starts about 10 minutes after mixing and is complete in about 45 minutes; but not fully set for 72 hours [73]. If plaster or gypsum is heated above 266 °F (130 °C), anhydrite is formed, which will also reform as gypsum if mixed with water [74]. Besides, fully set plaster mold is able to absorb water from precipitates because of its porosity, which made it an idea mold material in this research.

3.2 Experiments

3.2.1 Materials and instruments

The materials used in this chapter are plaster of Paris, kaolinite clay, DI water and plastic card. The plaster of Paris is from DAP products Inc.; which product code is 10304. This kaolinite clays has plastic limit of 33%. E64i1s Sartorius analytical balance and Fowler electronic digital caliper, model 53-100-004-2, are used to control materials ratio and measure parameters. Hitachi S-4800 Field Emission Scanning Electron Microscope was used to characterize the morphology changes during molding processing.

3.2.2 Experiment methods

Specimen design

Specimens were designed as Figure 3.1 which also illustrate the dimensions (in mm). The shape and parameters are based on the standard of tensile specimens. The amount of polymers was not much for big size specimens.

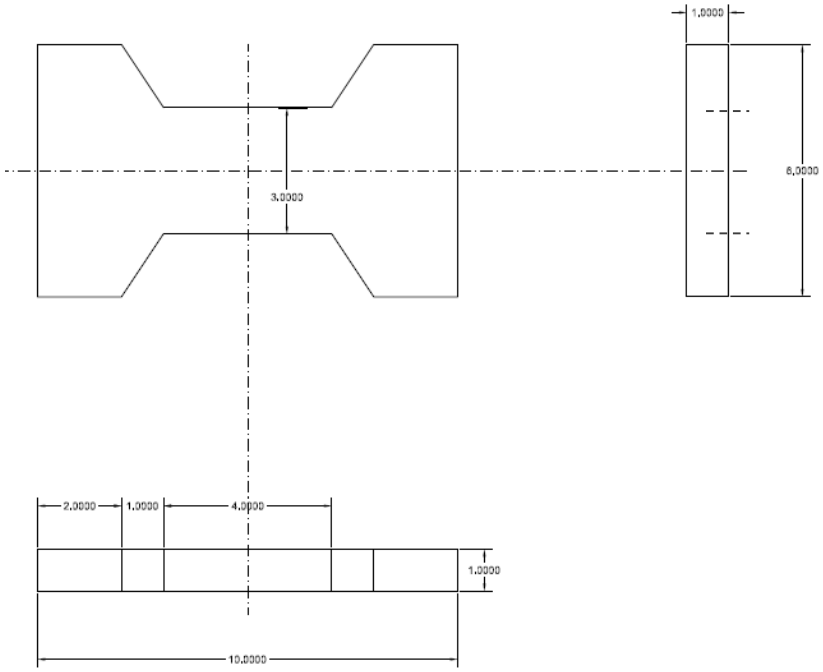

Figure 3.1. Three view drawing of specimen design

As shown in Figure 3.1, the test area is 4 mm × 3 mm rectangle and thickness is 1 mm.

Mold making

Plastic card which was 1 mm thick was carved by a knife into the designed shape. Kaolinite and water were mixed at plastic limit of 33%. Clays were fill into groove of plastic mold carved in former step. Five of dog-bone-shape clay pieces are put on dust-free kim wipers in a petri dish and dried at room temperature in vacuum oven for one hours. Plaster of Paris

powder was mixed into water at ratio of 2:1 and slowly poured over clay bottom mold to prevent bubbles. The plaster molds were cured in 20 min and washed to clean kim wiper and clays after 24 settled. Molds were fully set 72 h after mixed.

Specimens molding

After the first fully filled and pressed of nHAP-PLGA-Collagen precipitate, specimens were left to dry for five minutes and added more precipitate to supplement the shrinked specimens. This step was repeat again and pressed tight with glass slides. Specimens are collected and put on glass slides after 20 min water absorption. Dog bone specimens are dried in vacuum oven under room temperature for 24 hours. The prepared specimens are stored in 4 $^{\circ}C$ in a refrigerator. One of the molds and specimens are exhibited in Figure 3.2.

Figure 3.2 One of plaster molds and dog bone specimens

All specimens are labeled, and their dimensions are measured by electronic digital caliper and recorded. Wideness and thickness are measured at three different position on every specimen. The average of three measurements are regarded as the dimensions of specimens.

Morphology characterization with SEM

Both nHAP-PLGA copolymers and nHAP-PLGA-Collagen block-polymers are characterized by Hitachi S-4800 Field Emission Scanning Electron Microscope under voltage of 2V, 5V and 10V and current of 10 μA.

3.3 Result and Discussion

3.3.1 Macro-scale measurement of nHAP-PLGA-Collagen specimens

The parameter records of specimens are listed in table 3.1.

Table 3.1. Dimensions of specimens measured by caliper

No.	wideness				thickness			
	50/50		75/25		50/50		75/25	
	Raw data	Ave.	Raw data	Ave.	Raw data	Ave.	Raw data	Ave.
	3.61		3.42		1.00		1.07	
1.00	3.54	3.50	3.39	3.46	1.00	0.96	1.01	1.00
	3.35		3.58		0.88		0.92	
	2.89		3.61		0.82		0.83	
2.00	2.78	2.90	3.52	3.58	0.71	0.77	0.73	0.77
	3.02		3.61		0.77		0.75	
	3.01		3.49		0.86		1.09	
3.00	2.86	2.93	3.80	3.61	0.79	0.84	1.04	1.04
	2.91		3.53		0.87		0.99	
	3.07		3.23		0.91		0.92	
4.00	2.84	2.92	3.23	3.18	0.81	0.85	0.93	0.90
	2.86		3.09		0.84		0.86	
	3.19		3.34		0.72		0.93	
5.00	2.98	3.08	3.35	3.36	0.74	0.73	0.73	0.86
	3.07		3.39		0.72		0.92	
	3.31		2.93		0.81		0.93	
6.00	3.33	3.33	3.17	3.02	0.82	0.81	0.97	0.95
	3.36		2.96		0.81		0.94	
	3.10		3.81		0.74		0.94	
7.00	3.04	3.08	3.69	3.73	0.79	0.75	1.00	0.92
	3.11		3.68		0.72		0.82	
	3.03		3.17		0.77		1.06	
8.00	2.98	3.02	3.27	3.23	0.64	0.72	1.05	0.99
	3.04		3.24		0.74		0.87	
	2.96		3.63		1.04		0.67	
9.00	3.28	3.09	3.80	3.71	0.93	0.93	0.72	0.71
	3.03		3.70		0.83		0.73	
	3.17		3.36		0.75		1.06	
10.00	3.17	3.12	3.40	3.38	0.74	0.74	1.01	1.05
	3.02		3.38		0.74		1.07	
	3.02		3.76		0.84		0.94	
11.00	3.07	3.02	3.42	3.56	0.87	0.84	0.95	0.99
	2.98		3.50		0.82		1.08	
	3.19		3.71		1.03		0.76	
12.00	3.26	3.20	3.58	3.65	1.03	1.00	0.86	0.83
	3.15		3.67		0.93		0.87	
	3.00		3.24		0.66		1.15	
13.00	2.96	2.98	3.47	3.38	0.70	0.70	1.08	1.06
	2.97		3.42		0.73		0.95	

	3.12		0.73	
14.00	3.02	3.10	0.68	0.70
	3.16		0.69	
	3.16		0.86	
15.00	3.16	3.23	0.84	0.88
	3.36		0.93	
	3.26		0.75	
16.00	3.34	3.38	0.77	0.76
	3.54		0.77	
	2.65		0.67	
17.00	2.63	2.67	0.67	0.75
	2.74		0.92	
	3.09		1.02	
18.00	3.19	3.18	0.92	0.91
	3.25		0.79	
	2.66		0.59	
19.00	2.47	2.53	0.65	0.61
	2.46		0.59	

Average values represented the dimensions of specimens. The wideness of specimens are 3.00 ∓ 0.50 mm, and the thickness are 1∓ 0.40 mm. 50/50 nHAP-PLGA-Collagen polymers have a larger amount to make more specimens, while 75/25 nHAP-PLGA-Collagen polymers are less. Due to the amount of polymer, 19 pieces of 50/50 nHAP-PLGA-Collagen specimens and 13 pieces of nHAP-PLGA-Collagen are collected in this step. Although parameters of dimensions varied, they keep in similar numerical. Errors from the difference could be corrected during tensile test by enter the real dimensions.

The appearance of 50/50 nHAP-PLGA-Collagen showed slightly yellowed compared to 75/25 block-polymer.

3.3.2 Micro-scale characterization on nHAP-PLGA-Collagen Polymer

As shown in Figure 3.3, SEM images revealed morphology changes to nHAP-PLGA-Collagen polymers. nHAP-PLGA copolymers in Figure 3.3 a) had no pores and shown no orientation preference. After decoration of collagen, polymers intended to self-assemble to sphere morphologies which diameters are about 200 nm and gathering together, meanwhile the loose structure introduced porosity characteristic to the polymer itself. Afterward, the applied mechanical pressure strengthens the loose structure. From Figure 3.3 d), the sphere morphology disappeared; however, the polymer itself kept porosity characteristic. Figure 3.3 c) further proved the polymer structure on a larger scale.

Porosity of polymer is another significant point for polymers applying as bone scaffold. Only with the complex cross-linked pores, can cells be seated and cultured in bone scaffolds. Though porosity brought reducing to mechanical properties, it has to be considered during mechanical tests.

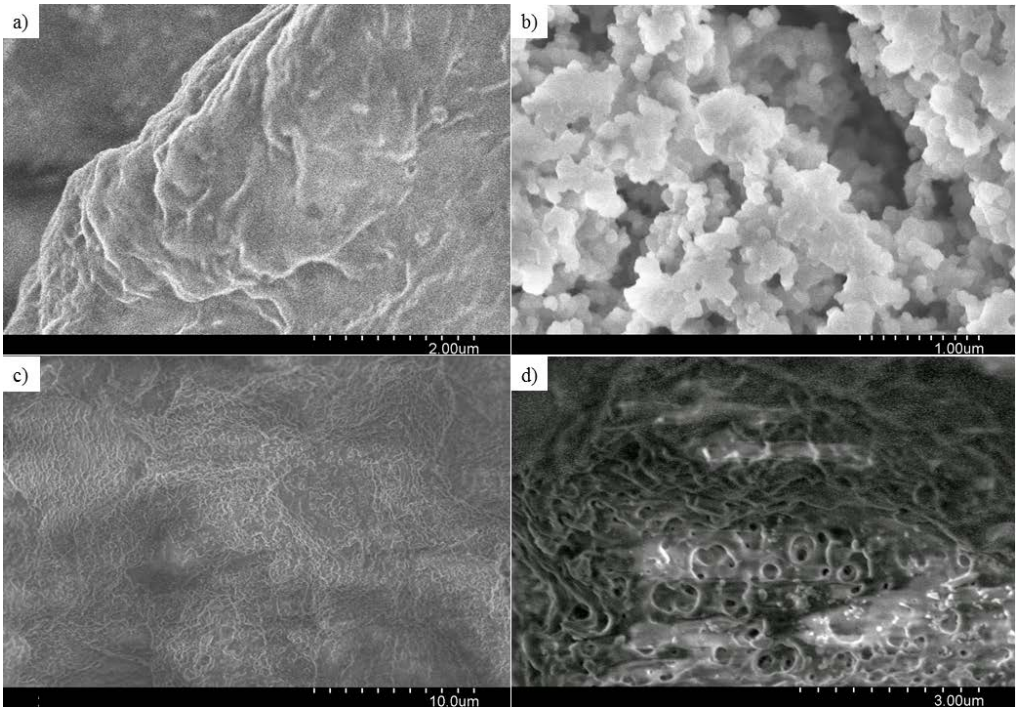

Figure 3.3. SEM images of a) nHAP-PLGA copolymers; b) unmolded nHAP-PLGA-Collagen block-polymers and c), d) molded nHAP-PLGA-Collagen block-polymers under different scales.

3.4 Conclusion

In this chapter, dog bone specimens are designed according to the amount of polymer and requirement for tensile tests. Bibulous uniform solid molds are made of gypsum plaster. And polymers are successfully molded. Test area is 4 mm × 3 mm rectangle and thickness is 1 mm. From micro-scale, nHAP-PLGA-Collagen polymers after molding process are becoming idea candidates for using as bone scaffold, since the present of porosity structure.

All specimens are measured and recorded. Though parameters slightly vary, this system error could be corrected by enter the real values during tensile test in next step.

Chapter 4

nHAP-PLGA-Collagen Degradation Study

4.1 Background

There are three major parameter sets in this study. Starting with time, though under different regenerated time, primary osteoblast proliferation is certainly determined at 24 hours, 3, 7, 14 and 21 days [69]. Therefore, a degradation monitor under 21 days is the basic standard to investigate degradation process, which was used in this chapter. And this test aimed at exploring the shelf-life and working- life of the two kinds of polymers under different environment. Specifically storage temperature at $4\,^{\circ}C$ and working temperature at $37\,^{\circ}C$ are set as one parameter; meantime, samples are soaked in PBS buffer solutions of pH 6.4, pH 7.4 and pH 8.4.

Degradation study are monitored and characterized by tensile test, Thermogravimetric Analysis (TGA), Fourier transform infrared spectroscopy (FTIR) and Scanning electron microscope (SEM). Those characterizations are basic three vital transformations for scaffold application during degradation. Tensile test focused on mechanical properties changes in the 21 days. Thermal decomposition temperature and transition are recorded by TGA, which indicate the possible phase change during 21-day degradation. FTIR which used for characterizing functional groups is used to investigate loss of functional group during degradation.

4.2 Experiments

4.2.1 Reagents and Instruments

The reagents and instruments used for experiments in this chapter are listed in table 4.1 and table 4.2.

Table 4.1 Information of reagents used in chapter 4

Reagents	Purity	Manufacturer	Other information
Sodium phosphate dibasic	98.0-102.0%	Sigma-Aldrich	

	heptahydrate		
Sodium	phosphate monobasic monohydrate	≥98%	Sigma-Aldrich
	DI water	/	/

Table 4.2 Information of instruments used in chapter 4

Instruments	Model/Cat. No.	Manufacturer
Advanced Hotplate Stirrer	11626262	Fisher Scientific
Waterproof pH Meter	ExStik	Extech
Analytical Balance	E64i1s	Sartorius
Thermogravimetric Analysis	Q500	TA Instruments
FT-IR Spectrometer	Nicolet iS50	Thermo Scientific
Field Emission Scanning Electron Microscope	S-4800	Hitachi
Tensile Testing Machine	5542	Instron
Explosion-Proof Refrigerator/Freezer	47747-226	VWR
Incubator	132000	Boekel Scientific
Electronic digital caliper, model	53-100-004-2	Fowler

4.2.2 Experiment Methods

Sample preparation

All specimens were labeled in last chapter. Taking temperature, pH, degradation time and monomer racial into consideration, specimens were divided in separate sets in Table 4.3.

Table 4.3. Specimen condition files

No.	Parameters	ratio 50/50	ratio 75/25
1.00	Duration time/d	0	0
	pH	7.4	7.4
	Temperature/$^{\circ}C$	4	4
2.00	Duration time/d	0	3
	pH	7.4	6.4
	Temperature/$^{\circ}C$	4	37
3.00	Duration time/d	0	3
	pH	7.4	7.4
	Temperature/$^{\circ}C$	4	37
4.00	Duration time/d	3	3
	pH	6.4	8.4
	Temperature/$^{\circ}C$	37	37

	Duration time/d	3	7
5.00	pH	7.4	6.4
	Temperature/$^{\circ}C$	37	37
	Duration time/d	3	7
6.00	pH	8.4	7.4
	Temperature/$^{\circ}C$	37	37
	Duration time/d	7	7
7.00	pH	6.4	8.4
	Temperature/$^{\circ}C$	37	37
	Duration time/d	7	14
8.00	pH	7.4	6.4
	Temperature/$^{\circ}C$	37	37
	Duration time/d	7	14
9.00	pH	8.4	7.4
	Temperature/$^{\circ}C$	37	37
	Duration time/d	14	14
10.00	pH	6.4	8.4
	Temperature/$^{\circ}C$	37	37
	Duration time/d	14	21
11.00	pH	7.4	6.4
	Temperature/$^{\circ}C$	37	37
	Duration time/d	14	21
12.00	pH	8.4	7.4
	Temperature/$^{\circ}C$	37	37
	Duration time/d	21	21
13.00	pH	6.4	8.4
	Temperature/$^{\circ}C$	37	37
	Duration time/d	21	
14.00	pH	7.4	
	Temperature/$^{\circ}C$	37	
	Duration time/d	21	
15.00	pH	8.4	
	Temperature/$^{\circ}C$	37	
	Duration time/d	3	
16.00	pH	7.4	
	Temperature/$^{\circ}C$	4	
	Duration time/d	7	
17.00	pH	7.4	
	Temperature/$^{\circ}C$	4	
	Duration time/d	14	
18.00	pH	7.4	
	Temperature/$^{\circ}C$	4	
	Duration time/d	21	
19.00	pH	7.4	
	Temperature/$^{\circ}C$	4	

In general, for 50/50 block-polymer, specimen No.1-3 are used as initial data. From specimen No.4 to No. 15 which later placed under $37^{\circ}C$, every 3 specimens were degraded under pH 6.4, pH 7.4 and pH 8.4 in order, as a set to test on day 3, day 7, day14 and day 21. Specimen No. 16, 17, 18 and 19 are stored at $4^{\circ}C$ and pH 7.4 and tested on day 3, day 7, day14 and day 21. 75/25 block-polymer specimens from No.2 to No. 13 shared the same treatment as 50/50 block-polymer, specimen No.4 to No. 15 did.

To keep pH, three kinds of 50 mM PBS buffer solutions were proportioned at pH 6.4, pH 7.4 and pH 8.4. 0.779 g $NaH_2PO_4 \cdot H_2O$ and 5.187 g $Na_2HPO_4 \cdot 7H_2O$ are completely dissolved in 500 mL DI water as 50 mM pH 7.4 PBS buffer. To prepare 50 mM pH 6.4 PBS buffer, 2.569 g $NaH_2PO_4 \cdot H_2O$ and 1.71 g $Na_2HPO_4 \cdot 7H_2O$ were dissolved in 500 mL DI water. And 0.098 g $NaH_2PO_4 \cdot H_2O$ along with 6.51 g $Na_2HPO_4 \cdot 7H_2O$ are solute for 500 mL 50mM pH 8.4 PBS buffer solution. All pH of solutions was verified by ExStik pH meter which had been calibrated with pH 4, pH 7 and pH 10 standard buffer solutions at accuracy of ±0.2.

PBS buffer solutions were added to the labeled petri dishes where samples were placed. Dishes were lidded up and sealed by para film. Same day testing samples, such as 75/25 No. 4, 5, 6 and 50/50 No. 2, 3, 4 on day 3, are packed in aluminum foil to avoid light effects and moisture lost. The samples under $37^{\circ}C$ were stayed in incubator. The $4^{\circ}C$ specimens were packed separately in refrigerator. Every time before tests, specimens were washed by DI water for three times, and vacuum dried at room temperature for 24 hours. All dimensions were measured again for tensile test and a knowledge of shrinkage.

Micro-scale degradation monitor by SEM

Both nHAP-PLGA copolymers and nHAP-PLGA-Collagen block-polymers are characterized by Hitachi S-4800 Field Emission Scanning Electron Microscope under voltage of 2V, 5V and 10V and current of 10 μA.

Mechanical properties tests

Tensile test was applied by 5542 Instron Tensile testing machine on day 3, day7, day 14 and day 21. Dimensions of test area were entered in Instron Merlin software. Extension rate was set at 2 mm/min. Elastic modulus was obtained from stress-strain plot graphs by calculating the slops at elastic deformation region which was linear tendency in stress-strain

plot graphs. Elastic modulus were recoded and graphed to analyze modulus changes during degradation.

FTIR characterization

The samples for FT-IR absorption spectra were collected at room temperature at wavelength of 4000-400 cm^{-1}. One background is collected before sample signals. Every spectra is repeatedly collected 32 times under ATR mode for high resolution. Omnic software suite attached to the FTIR instrument was used for spectrum's analysis. Tests were taken on day 3, day 7, day 14 and day 21.

Thermogravimetric Analysis profiles establishment

The TGA could measure the mass range between 1mg to 1g. Samples were collected around 20 mg and heating up in platinum pan under nitrogen atmosphere. Ramp procedure was used in thermal behavior analysis, heating rate at 5 from room temperature to 600. Tests were taken on day 3, day 7, day 14 and day 21.

4.3 Result and Discussion

4.3.1 SEM Degradation Monitor

On micro-scale, the major change happened on pores. The pores vanished during the degradation. In Figure 4.1 a), the 75/25 polymer had a porous structure with pores size from 200 nm to 2 μm, which was suitable for cells to seed in. Later in Figure 4.1 b), on the third day of degradation, the amount of pores diminished significantly. And finally, on the seventh day, there is no obvious existence of porous structure any more. 50/50 polymer had nearly the same phenomenon during degradation. Therefore, the disappearance of porous structure is a major change in early stage of nHAP-PLGA-Collagen block-polymer degradation.

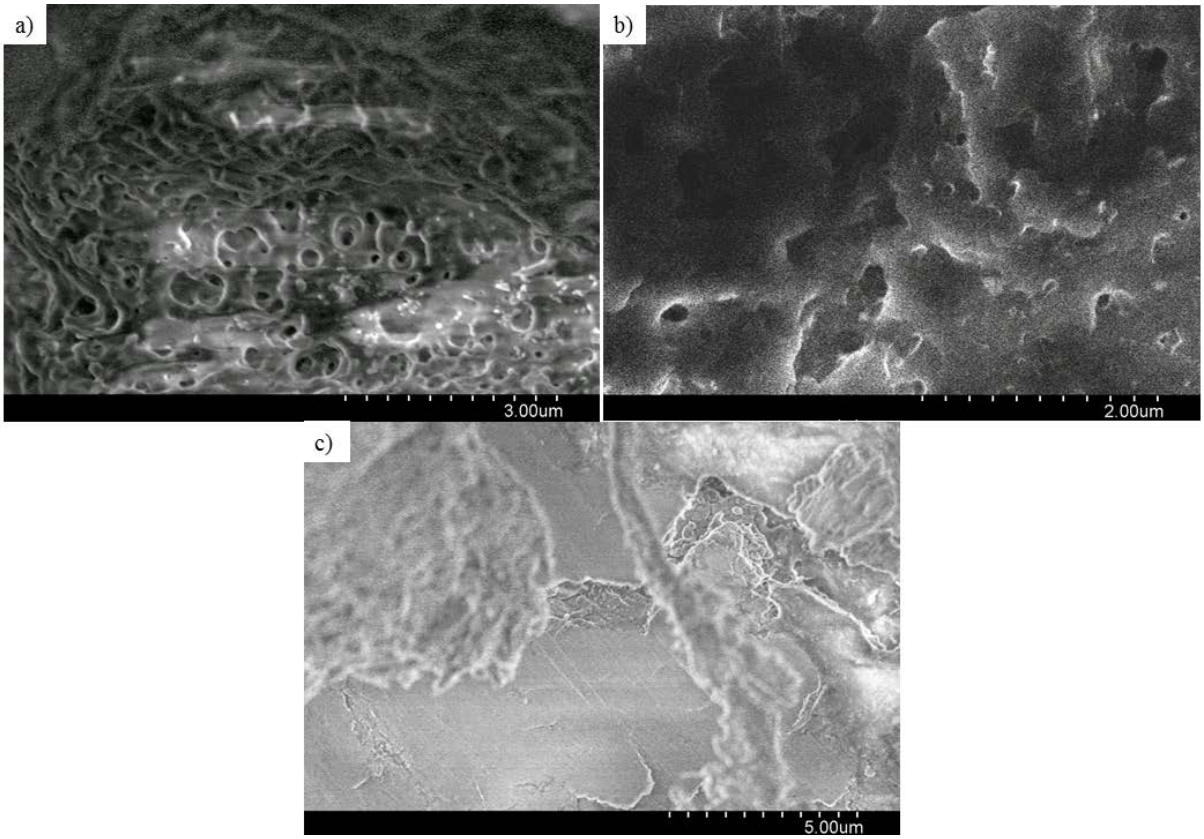

Figure 4.1. SEM image of a) 75/25 polymer specimen on day 0, b) 75/25 polymer specimen on day 3 and c) 75/25 polymer specimen on day 7.

4.3.2 Mechanical Properties

A typical tensile testing graph is shown in Figure 4.2. The section from 0 to point a is elastic deformation area. Specimens went through an elastic deformation and would recover if unload before point a. The slope of linear function is the elastic modulus of each specimen. However, according to the system error of machine, the results should be multiplied by 2 Following section from point a to b is plastic deformation area which deformation could not recover any more. Point of intersection between the curve and a vertical line to x-axis at b represent ultimate tensile strength. Necking happened in section from point b to point c and fracture at point c.

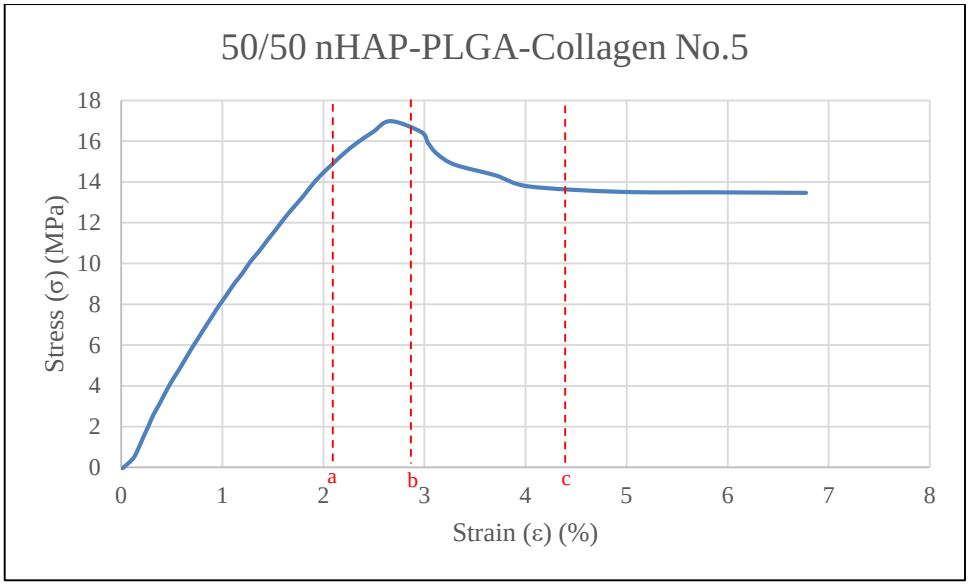

Figure 4.2. Tensile testing stress-strain graph of 50/50 nHAP-PLGA-Collagen No.5

During the degradation treatment in 21 days, stress-strain graphs of all 32 specimens has been collected for elastic modulus and ultimate tensile strength calculation. Tendency of elastic modulus and ultimate tensile strengths are recorded in Figure 4.2. Those curves represented the mechanical property losses during degradation.

Over all, the specimens stored at $4^{\circ}C$ are the most stable samples. Modulus stayed about same at 10-12 MPa, and ultimate tensile strength was as high as 6.6 MPa on the 21st day. Compare to this, other factors during degradation had less impact to specimens. Form the result of tensile tests, temperature is the major factor which influence shelf-life of nHAP-PLGA-Collagen bone scaffold.

Mechanical properties for some specimens, including elastic modulus of all 50/50 nHAP-PLGA-Collagen specimens and all ultimate tensile strength except 75/25, $37^{\circ}C$ of pH 7.6 and 8.4, increased from day 0 to day 3. Combine with Figure 4.1, the collapsing of pores was the reason why mechanical properties increased. Without those pores, polymers bonded more close and strengthened the mechanical properties of specimens.

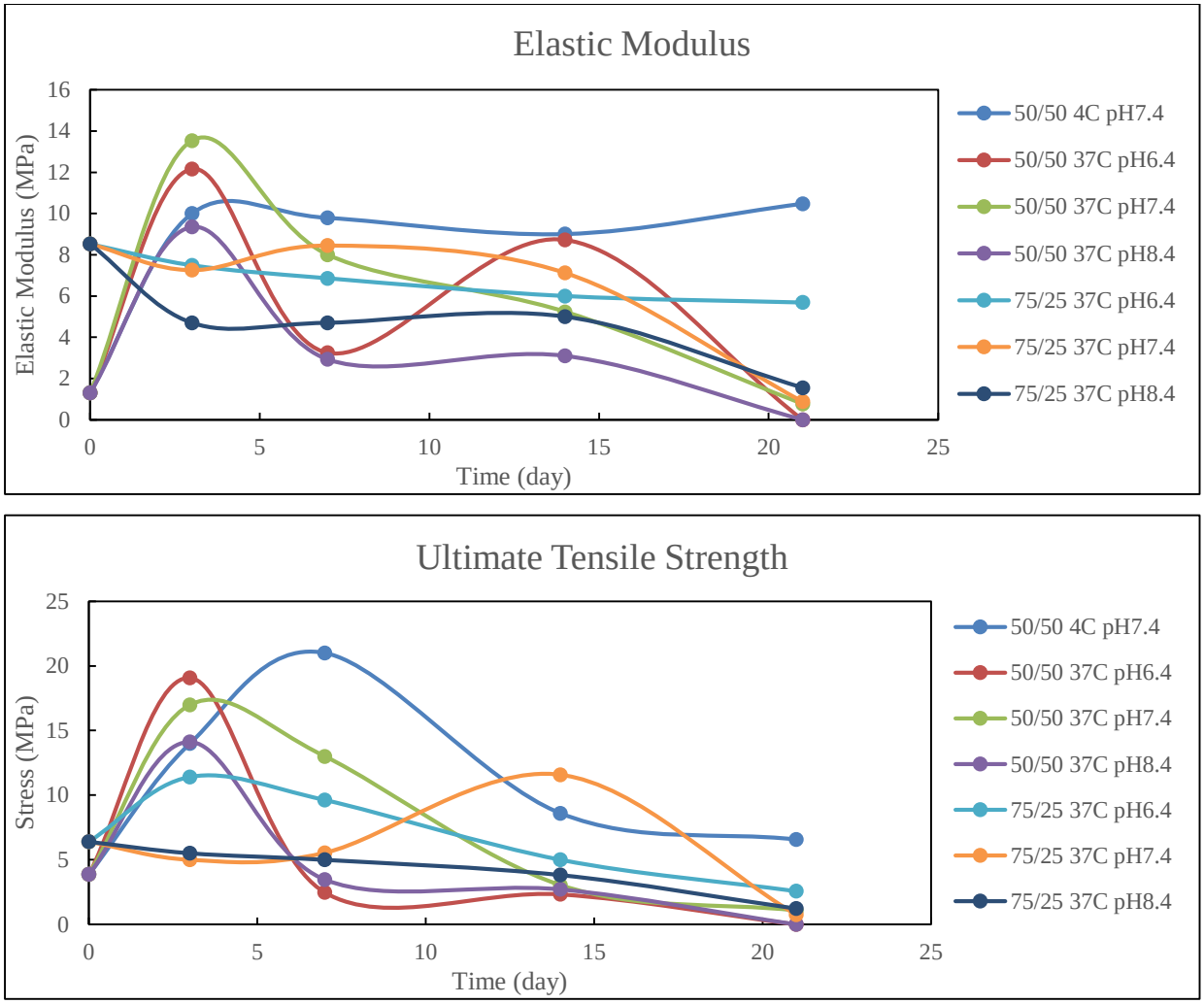

Figure 4.3. Elastic modulus and ultimate tensile strength tendency coordinate graphs.

Comparing those two kinds of polymers, 75/25 nHAP-PLGA-Collagen polymer was more stable than the polymer of 50/50 monomers during the whole degradation process. And at the end, on 21st day, all 75/25 polymeric specimens were still able to be tested, while 50/50 specimens became too fragile for tensile tests. In the test on 21st day, those 50/50 specimens have cracked and fractured once clamps applied. In another word, the polymers of 75/25 monomer ratio stayed a longer time in degradation experiments.

Three pH values of 6.4, 7.4 and 8.4 were compared separately on 75/25 nHAP-PLGA-Collagen and 50/50 nHAP-PLGA-Collagen. For 50/50 nHAP-PLGA-Collagen, specimens in pH 7.4 solution generally have the highest elastic modulus during degradation. Specimen in pH 6.4 has been high once on the 14th day due to variation of specimens. From ultimate tensile strength graph, the same conclusion could be recapped. Moreover, specimen in pH 7.4 solutions was the only one testable. On the other hand, polymer in pH 8.4 solution are always the most fragile specimens, which means although both acidic and alkaline environment

speeded up degradation, higher pH brought a more severe impact. Seeing tendency of 75/25 nHAP-PLGA-Collagen, alkaline environment has still been the most severe environment for keeping this bone scaffold material. Samples under pH 6.4 and pH 7.4 were hard to compare, which could know from further investigation using TGA and FTIR.

4.3.3 TGA Profiles

Typical TGA profiles of nHAP-PLGA-Collagen are illustrate in chapter 2, which have two ramps: The first major ramp represents phase transition of nHAP-PLGA blocks and depolymerization. And the second minor ramp started around $380\,^{\circ}C$ represent decomposition of collagen. During the 21-day degradation, the basic shapes were stayed the same. The position of major ramps moved to a lower temperature while the position minor ramps stayed the same. An example was shown in Figure 4.4. In Figure 4.4 a), b) for 50/50 polymer, though no change on percentage of first ramps, the start points of first transition lowered from initial $253.67\,^{\circ}C$ to $236.87\,^{\circ}C$ after 21 days. DTA Peak also reveal the change of major transition, from $277.00\,^{\circ}C$ to $258.12\,^{\circ}C$ diminished nearly $20\,^{\circ}C$. However, the secondary transition did not have significant change on ramp position; instead, the percentage of secondary ramp increased. Polymers had a further phase separation after 21-day degradation. 75/25 polymer has the same tendency to 50/50 polymer. In Figure 4.4 c), d), major transition starting points changed from $262.55\,^{\circ}C$ to $233.74\,^{\circ}C$ and DTA peaks changed from $296.37\,^{\circ}C$ to 259.57. Secondary ramps have still kept at the same position but weight changed less, from 5.005% to 6.695% around 1.7%.

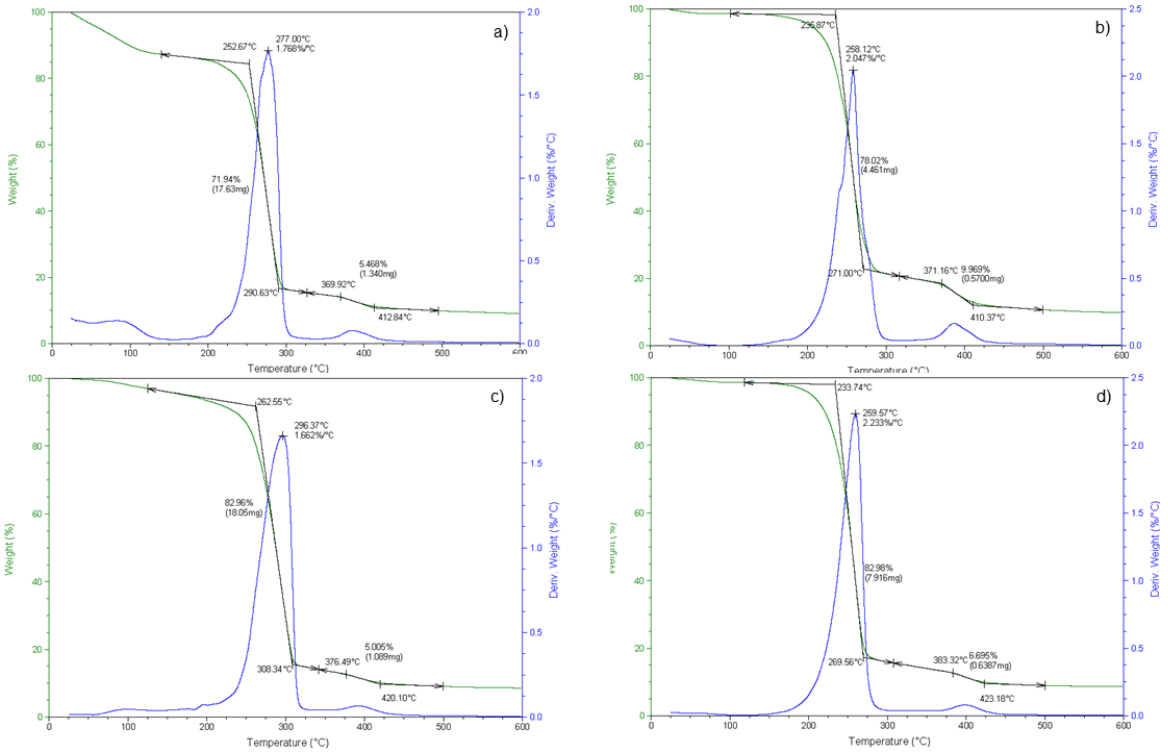

Figure 4.4. TGA profile comparison of D0 and D21: a) 50/50 nHAP-PLGA-Collagen D0, b) 50/50 nHAP-PLGA-Collagen pH 7.4 D21, c) 75/25 nHAP-PLGA-Collagen D0, d) 75/25 nHAP-PLGA-Collagen pH 7.4 D21

All parameters were recorded and graphed to show and compare the tendency during degradation. Figure 4.5. gave the further proof to explain the phase separation and degradation states. Seeing the tendency of first ramp starting point, polymers generally intended to started to decomposition at a lower temperature during the 21 days. Compare to $0\,^{\circ}C$, pH 7.4, 50/50 polymers, $37\,^{\circ}C$, pH 6.4, 75/25 polymers and $37\,^{\circ}C$, pH 6.4, 50/50 polymers, the other specimens had a greater change on phase transition temperature. The same tendency of peak movement in DTA profiles complementary proved this was not accidental. 50/50 polymers had a larger move from a higher initial temperature, which means a deeper degradation on the polymer. A slightly acidic environment for both kinds of polymers are easier for preserving this kind of bone scaffold polymeric material.

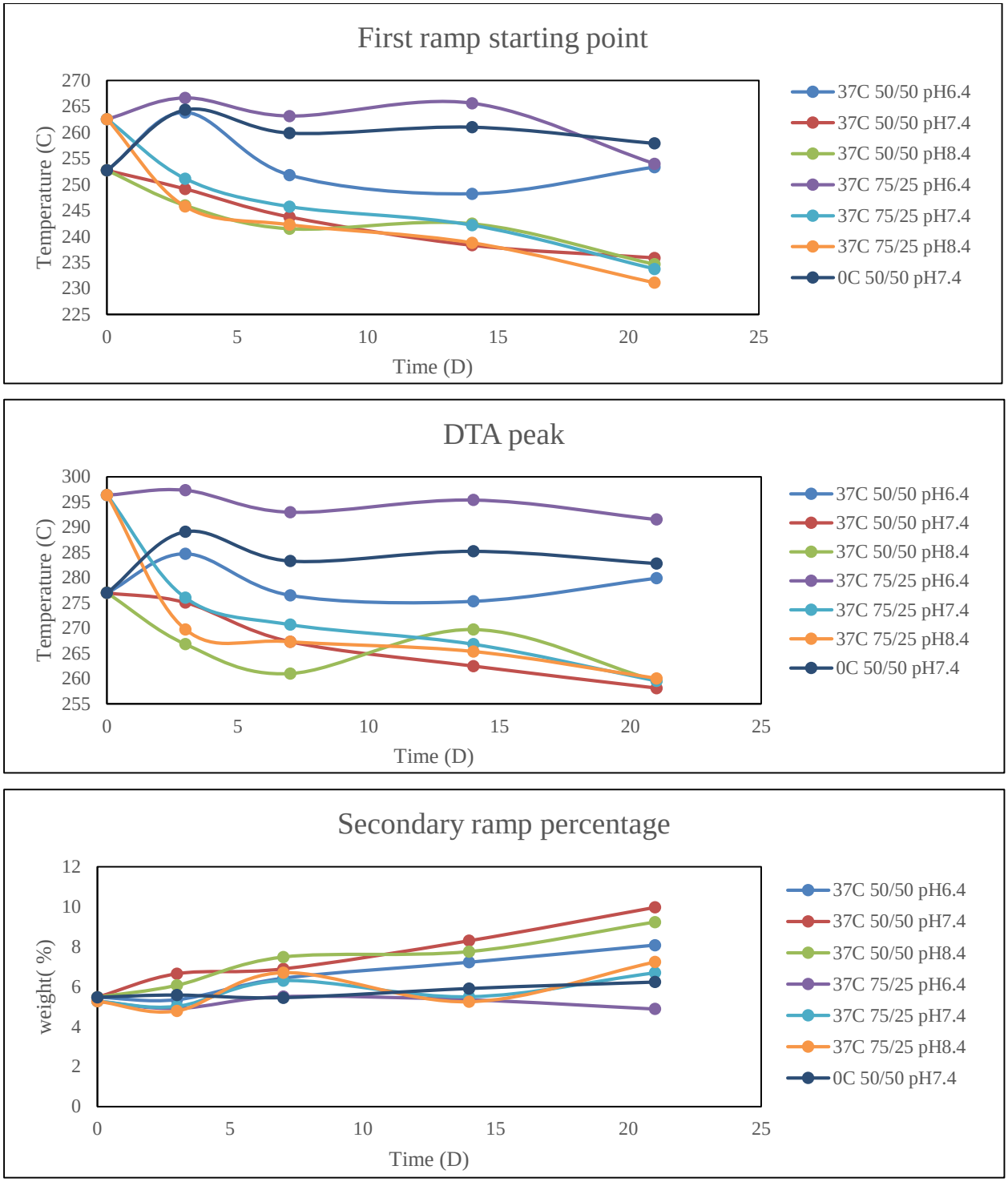

Figure 4.5. Graphs of decomposition temperature move and secondary ramp percentage change

50/50 polymers had the most significant increasing percentage on secondary ramp in Figure 4.5. The secondary ramp was caused by phase separation during degradation. This rising weight of second phase represent the degree of degradation.

According to TGA profiles of polymers in 21-day degradation, temperature was still a decisive factor. The low temperature would keep a longer shelf life for this bone scaffold

material. Secondly, 75/25 polymer has a relatively higher stability than 50/50 polymer, which kept the same pattern as regular PLGA polymers stated in the first chapter. Alkaline environment is destructive to nHAP-PLGA-Collagen. All specimens in pH 8.4 had a higher degree of degradation, while neutral and acidic environment samples performed better. Samples in acidic environment are even comparable to specimens stored under 4 $^{\circ}C$. This character fits the characteristic of healing bone environment in neutral or acidic environment.

4.3.4 FTIR Spectra

FTIR spectra was using to monitor variation of functional groups during degradation. Results of 75/25 block polymer did not show obvious regular variations. On the other hand, spectra of 50/50 polymers had noticeable appeared and disappeared peaks on spectra. In Figure 4.6 b), 50/50 polymers stored at 4 $^{\circ}C$ did not have changes, which strengthened the point that temperature is a decisive factor in degradation. And the spectra could regard as standard to identify peak variations.

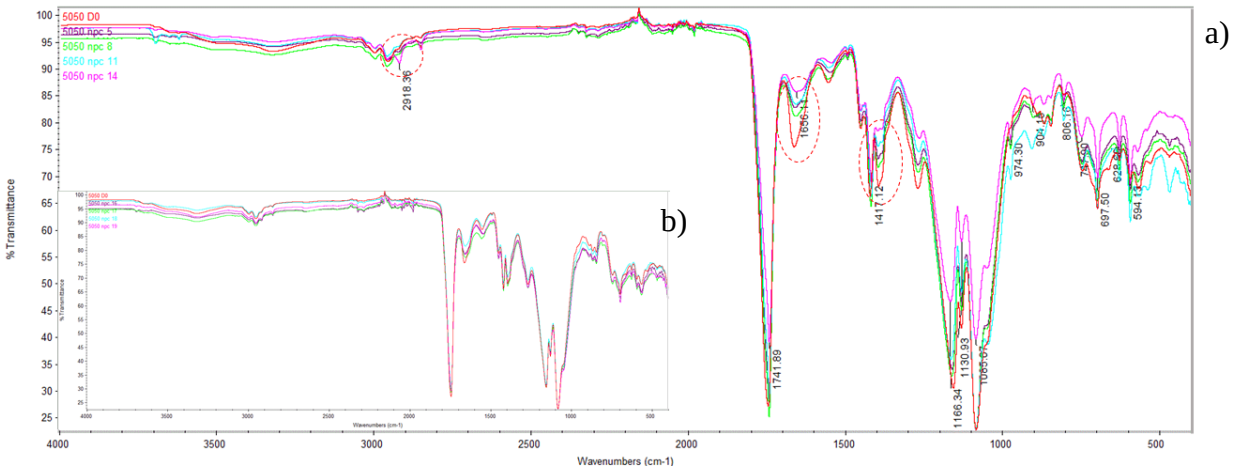

Figure 4.6. FTIR spectra of a) 37 $^{\circ}C$, pH 7.4, 50/50 polymer on day 0, day 3, day 7, day14, day21; b)) 0 $^{\circ}C$, pH 7.4, 50/50 polymer on day 0, day 3, day 7, day14, day21

In Figure 4.6 a), compared to original spectrum, a peak at 2918 cm^{-1} appeared, and correspondingly, peak 1656 cm^{-1} and 1417 cm^{-1} gradually disappeared. The present of 2918 cm^{-1} in this kind of block polymer represent the appearance of –COOH. This means some of the ester bond which formed by condensation polymerization has been broken. Peak 1656 cm^{-1} along with 1417 cm^{-1} which are also decreased in 75/25 spectra represent the decreasing of unsaturated –C-CH_2 bonds. Without distinctly extra nor absent peak among each spectrum in different pH environment, the factor of pH could not be evaluated through FTIR analysis.

4.4 Conclusion

In this chapter, degradation was monitored by several techniques. From SEM image and tensile test results, nHAP-PLGA-Collagen polymers are porous materials with micron scale pores. These pores collapsed and disappeared in early stage of degradation, which increasing mechanical properties such as ultimate tensile strength and elastic modulus. However, as degradation further going on, mechanical properties began to decrease. Combined with the results from TGA and FTIR, temperature is a decisive factor that the specimens under 4 $^{\circ}C$ has barely degraded. Comparing two kinds of polymers, 75/25 nHAP-PLGA-Collagen block polymer has a higher stability than the polymer in D,L-lactide and glycolide monomer ratio of 50:50, keeping the same regulation as unmodified PLGA did. Potential of Hydrogen as an environmental factor could not be judged by using FTIR; however, from both mechanical tests and TGA profiles, alkaline environment would accelerate speed of degradation, and neutral or acidic environments is better for keeping this kind of bone scaffold material. For 75/25 block polymer, in most case, buffer solution of pH 6.4 kept specimens even better than that of pH 7.4. Polymers in monomer ratio of 50/50 are completely lost their mechanical properties after 21days conversely verified the chosen duration is suitable for degradation investigating on this novel synthesized polymer. The degradation rate of this polymer is adaptable by adjusting monomer ratio before polymerization and control external factors as temperature and pH values.

Further research could base on a bionic environment by adding enzymes and other components of tissue fluid. Collagen, as a main component of bone tissue could be dissolved by enzymes and other protein balls in vivo. Another problem need to be discuss is that whether will the increasing mechanical properties from bone formation be able to complement the loss strength from polymer degradation and support normal lives for patients.

References:

1. Liu, X. and P.X. Ma, *Polymeric scaffolds for bone tissue engineering.* Annals of biomedical engineering, 2004. **32**(3): p. 477-486.
2. Burchardt, H., *The biology of bone graft repair.* Clinical orthopaedics and related research, 1983. **174**: p. 28-34.
3. Gutierrez, G.E., et al., *Transdermal lovastatin enhances fracture repair in rats.* Journal of Bone and Mineral Research, 2008. **23**(11): p. 1722-1730.
4. Chung, K.C. and S.V. Spilson, *The frequency and epidemiology of hand and forearm fractures in the United States.* The Journal of hand surgery, 2001. **26**(5): p. 908-915.
5. Liao, S., et al., *Hierarchically biomimetic bone scaffold materials: nano - HA/collagen/PLA composite.* Journal of Biomedical Materials Research Part B: Applied Biomaterials, 2004. **69**(2): p. 158-165.
6. Rezwan, K., et al., *Biodegradable and bioactive porous polymer/inorganic composite scaffolds for bone tissue engineering.* Biomaterials, 2006. **27**(18): p. 3413-3431.
7. Chaikof, E.L., et al., *Biomaterials and scaffolds in reparative medicine.* Annals of the New York Academy of Sciences, 2002. **961**(1): p. 96-105.
8. Hench, L.L., *Bioceramics, a clinical success.* American Ceramic Society Bulletin, 1998. **77**(7): p. 67-74.
9. Hench, L.L., *Bioceramics: from concept to clinic.* Journal of the American Ceramic Society, 1991. **74**(7): p. 1487-1510.
10. Lobel, K. and L. Hench, *In-vitro protein interactions with a bioactive gel-glass.* Journal of Sol-Gel Science and Technology, 1996. **7**(1-2): p. 69-76.
11. Lobel, K. and L. Hench, *In vitro adsorption and activity of enzymes on reaction layers of bioactive glass substrates.* Journal of biomedical materials research, 1998. **39**(4): p. 575-579.
12. Ohgushi, H., et al., *Osteogenic differentiation of cultured marrow stromal stem cells on the surface of bioactive glass ceramics.* Journal of biomedical materials research, 1996. **32**(3): p. 341-348.
13. Day, R.M., et al., *Assessment of polyglycolic acid mesh and bioactive glass for soft-tissue engineering scaffolds.* Biomaterials, 2004. **25**(27): p. 5857-5866.
14. Keshaw, H., A. Forbes, and R.M. Day, *Release of angiogenic growth factors from cells encapsulated in alginate beads with bioactive glass.* Biomaterials, 2005. **26**(19): p. 4171-4179.
15. Schepers, E., et al., *Bioactive glass particulate material as a filler for bone lesions.* Journal of oral rehabilitation, 1991. **18**(5): p. 439-452.
16. Gatti, A., G. Valdre, and Ö. Andersson, *Analysis of the in vivo reactions of a bioactive glass in soft and hard tissue.* Biomaterials, 1994. **15**(3): p. 208-212.
17. Roether, J., et al., *Novel bioresorbable and bioactive composites based on bioactive glass and polylactide foams for bone tissue engineering.* Journal of materials science: materials in medicine, 2002. **13**(12): p. 1207-1214.
18. Xynos, I.D., et al., *Ionic products of bioactive glass dissolution increase proliferation of human osteoblasts and induce insulin-like growth factor II mRNA expression and protein synthesis.* Biochemical and biophysical research communications, 2000. **276**(2): p. 461-465.
19. Xynos, I., et al., *Bioglass® 45S5 stimulates osteoblast turnover and enhances bone formation in vitro: implications and applications for bone tissue engineering.* Calcified

Tissue International, 2000. **67**(4): p. 321-329.
20. Hench, L.L. and J. Wilson, *An introduction to bioceramics*. Vol. 1. 1993: World Scientific.
21. Best, S., et al., *Bioceramics: past, present and for the future.* Journal of the European Ceramic Society, 2008. **28**(7): p. 1319-1327.
22. Yamamuro, T., L.L. Hench, and J. Wilson, *CRC Handbook of Bioactive Ceramics: Bioactive glasses and glass-ceramics; Vol. 2, Calcium Phosphate and Hydroxylapatite ceramics*. 1990: CRC press.
23. LeGeros, R.Z. and J.P. LeGeros. *Calcium phosphate bioceramics: past, present and future*. in *Key Engineering Materials*. 2002. Trans Tech Publ.
24. Seal, B., T. Otero, and A. Panitch, *Polymeric biomaterials for tissue and organ regeneration.* Materials Science and Engineering: R: Reports, 2001. **34**(4): p. 147-230.
25. Di Martino, A., M. Sittinger, and M.V. Risbud, *Chitosan: a versatile biopolymer for orthopaedic tissue-engineering.* Biomaterials, 2005. **26**(30): p. 5983-5990.
26. Lee, S.B., et al., *Study of gelatin-containing artificial skin V: fabrication of gelatin scaffolds using a salt-leaching method.* Biomaterials, 2005. **26**(14): p. 1961-1968.
27. Mohanty, A., M. Misra, and G. Hinrichsen, *Biofibres, biodegradable polymers and biocomposites: an overview.* Macromolecular materials and Engineering, 2000. **276**(1): p. 1-24.
28. Mano, J.F., et al., *Bioinert, biodegradable and injectable polymeric matrix composites for hard tissue replacement: state of the art and recent developments.* Composites Science and Technology, 2004. **64**(6): p. 789-817.
29. Ratner, B.D., et al., *Biomaterials science: an introduction to materials in medicine*. 2004: Academic press.
30. Jagur-Grodzinski, J., *Biomedical application of functional polymers.* Reactive and Functional Polymers, 1999. **39**(2): p. 99-138.
31. Dunn, A.S., P.G. Campbell, and K.G. Marra, *The influence of polymer blend composition on the degradation of polymer/hydroxyapatite biomaterials.* Journal of Materials Science: Materials in Medicine, 2001. **12**(8): p. 673-677.
32. Heidemann, W., et al., *Degradation of poly (D, L) lactide implants with or without addition of calciumphosphates in vivo.* Biomaterials, 2001. **22**(17): p. 2371-2381.
33. Martin, C., H. Winet, and J. Bao, *Acidity near eroding polylactide-polyglycolide in vitro and in vivo in rabbit tibial bone chambers.* Biomaterials, 1996. **17**(24): p. 2373-2380.
34. Yang, S., et al., *The design of scaffolds for use in tissue engineering. Part I. Traditional factors.* Tissue engineering, 2001. **7**(6): p. 679-689.
35. Eitan, A., et al., *Surface modification of multiwalled carbon nanotubes: toward the tailoring of the interface in polymer composites.* Chemistry of Materials, 2003. **15**(16): p. 3198-3201.
36. Zhu, J., et al., *Reinforcing epoxy polymer composites through covalent integration of functionalized nanotubes.* Advanced Functional Materials, 2004. **14**(7): p. 643-648.
37. Bhuiyan, D., et al., *Novel synthesis and characterization of a collagen-based biopolymer initiated by hydroxyapatite nanoparticles.* Acta biomaterialia, 2015. **15**: p. 181-190.
38. Suchanek, W. and M. Yoshimura, *Processing and properties of hydroxyapatite-based biomaterials for use as hard tissue replacement implants.* Journal of Materials Research, 1998. **13**(01): p. 94-117.
39. Porjazoska, A., et al., *Synthesis and characterization of poly (ethylene glycol)-poly (D, L-lactide-co-glycolide) poly (ethylene glycol) tri-block co-polymers modified with collagen: a model surface suitable for cell interaction.* Journal of Biomaterials Science, Polymer Edition, 2006. **17**(3): p. 323-340.

40. Horisaka, Y., et al., *Histological changes of implanted collagen material during bone induction.* Journal of biomedical materials research, 1994. **28**(1): p. 97-103.
41. Rovira, A., et al., *Colonization of a calcium phosphate/elastin-solubilized peptide-collagen composite material by human osteoblasts.* Biomaterials, 1996. **17**(15): p. 1535-1540.
42. Yoshimoto, H., et al., *A biodegradable nanofiber scaffold by electrospinning and its potential for bone tissue engineering.* Biomaterials, 2003. **24**(12): p. 2077-2082.
43. Kim, S.Y. and G.T.R. Palmore, *Conductive hydrogel for bio-electrocatalytic reduction of dioxygen.* Electrochemistry Communications, 2012. **23**: p. 90-93.
44. Edward, G.X., *Is trabecular bone tissue different from cortical bone tissue?* Forma, 1998. **12**(3): p. 185-196.
45. Zysset, P.K., et al., *Elastic modulus and hardness of cortical and trabecular bone lamellae measured by nanoindentation in the human femur.* Journal of biomechanics, 1999. **32**(10): p. 1005-1012.
46. Bayraktar, H.H., et al., *Comparison of the elastic and yield properties of human femoral trabecular and cortical bone tissue.* Journal of biomechanics, 2004. **37**(1): p. 27-35.
47. Roeder, B.A., et al., *Tensile mechanical properties of three-dimensional type I collagen extracellular matrices with varied microstructure.* Journal of biomechanical engineering, 2002. **124**(2): p. 214-222.
48. Mima, S., et al., *Highly deacetylated chitosan and its properties.* Journal of Applied Polymer Science, 1983. **28**(6): p. 1909-1917.
49. Yin, Y.J., et al., *Properties of polyelectrolyte complex films of chitosan and gelatin.* Polymer international, 1999. **48**(6): p. 429-432.
50. Zhang, Y., et al., *Electrospinning of gelatin fibers and gelatin/PCL composite fibrous scaffolds.* Journal of Biomedical Materials Research Part B: Applied Biomaterials, 2005. **72**(1): p. 156-165.
51. Manolagas, S.C., *Birth and death of bone cells: basic regulatory mechanisms and implications for the pathogenesis and treatment of osteoporosis 1.* Endocrine reviews, 2000. **21**(2): p. 115-137.
52. Frost, H.M., *Bone remodeling and its relationship to metabolic bone diseases*. 1973: Charles C. Thomas Publisher.
53. Cho, T.J., L.C. Gerstenfeld, and T.A. Einhorn, *Differential temporal expression of members of the transforming growth factor β superfamily during murine fracture healing.* Journal of Bone and Mineral Research, 2002. **17**(3): p. 513-520.
54. Einhorn, T.A., *The cell and molecular biology of fracture healing.* Clinical orthopaedics and related research, 1998. **355**: p. S7-S21.
55. Reddi, A., *Bone morphogenetic proteins: from basic science to clinical applications.* J Bone Joint Surg Am, 2001. **83**(1 suppl 1): p. S1-S6.
56. Sandberg, M., H. Aro, and E. Vuorio, *Gene expression during bone repair.* Clinical orthopaedics and related research, 1993(289): p. 292-312.
57. Ferguson, C., et al., *Does adult fracture repair recapitulate embryonic skeletal formation?* Mechanisms of development, 1999. **87**(1): p. 57-66.
58. Dimitriou, R., E. Tsiridis, and P.V. Giannoudis, *Current concepts of molecular aspects of bone healing.* Injury, 2005. **36**(12): p. 1392-1404.
59. Carter, D., M. Van der Meulen, and G. Beaupre, *Mechanical factors in bone growth and development.* Bone, 1996. **18**(1): p. S5-S10.
60. Heckman, J.D. and R.W. Bucholz, *Rockwood and Green's fractures in adults*. 2001: Lippincott Williams & Wilkins.
61. Mckibbin, B. *The biology of fracture healing in long bones*. in *J Bone Joint Surg [Br*. 1978. Citeseer.

62. Gerstenfeld, L.C., et al., *Fracture healing as a post‐natal developmental process: Molecular, spatial, and temporal aspects of its regulation.* Journal of cellular biochemistry, 2003. **88**(5): p. 873-884.
63. Kon, T., et al., *Expression of Osteoprotegerin, Receptor Activator of NF‐κB Ligand (Osteoprotegerin Ligand) and Related Proinflammatory Cytokines During Fracture Healing.* Journal of Bone and Mineral Research, 2001. **16**(6): p. 1004-1014.
64. Brighton, C.T. and R.M. Hunt, *Early histological and ultrastructural changes in medullary fracture callus*. J Bone Joint Surg Am, 1991. **73**(6): p. 832-847.
65. Laurencin, C.T., et al., *Tissue engineered bone-regeneration using degradable polymers: the formation of mineralized matrices.* Bone, 1996. **19**(1): p. S93-S99.
66. Huang, Y., et al., *In vitro and in vivo evaluation of akermanite bioceramics for bone regeneration.* Biomaterials, 2009. **30**(28): p. 5041-5048.
67. Petite, H., et al., *Tissue-engineered bone regeneration.* Nature biotechnology, 2000. **18**(9): p. 959-963.
68. Hulbert, S., et al., *Potential of ceramic materials as permanently implantable skeletal prostheses.* Journal of biomedical materials research, 1970. **4**(3): p. 433-456.
69. Cima, L., et al., *Tissue engineering by cell transplantation using degradable polymer substrates.* Journal of biomechanical engineering, 1991. **113**(2): p. 143-151.
70. Wu, L. and J. Ding, *In vitro degradation of three-dimensional porous poly (D, L-lactide-co-glycolide) scaffolds for tissue engineering.* Biomaterials, 2004. **25**(27): p. 5821-5830.
71. Zhang, R. and P. Ma. *Composite scaffolds for bone tissue engineering: degradation*. in *47th Annual Meeting, Orthopaedic Research Society, San Francisco, CA*. 2001.
72. Davis, J.R., *Tensile testing*. 2004: ASM international.
73. Schmidt, V.E., J.H. Somerset, and R.E. Porter, *Mechanical properties of orthopedic plaster bandages.* Journal of biomechanics, 1973. **6**(2): p. 173-185.
74. Deer, W., R. Howie, and J. Zussman, *An introduction to rock forming materials*. 1992, Longman, London.